

---

# Spin dependent tunneling in spintronics nanostructures



By

**Faizan Ahmed**

(123-FBAS/MSPHY/F12)

**Supervisor:**

**Dr. Naeem Ahmed**

Assistant Professor

Department of Physics, FBAS,

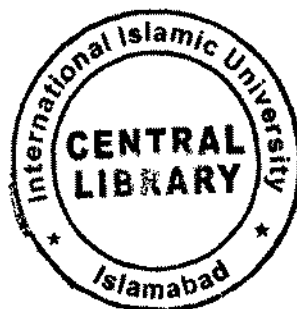
IIUI

**Department of Physics**

**Faculty of Basic and Applied Sciences**

**International Islamic University, Islamabad**

**(2015)**



TH-14635 K/S/  
Accession No 14635

MS  
621.381

FAS

- Spintronics
- Spin tunneling
- Magnetoresistance.

---

# Spin dependent tunneling in spintronics nanomaterials

By:


**Faizan Ahmed**

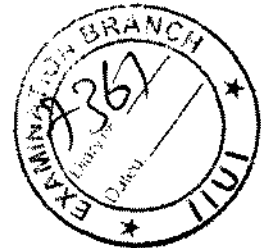
(123-FBAS/MSPHY/F12)

This Thesis is submitted to Department of Physics International Islamic University,  
Islamabad for the award of degree of MS Physics.

  
Chairman Department of Physics

International Islamic University Islamabad

  
Dean Faculty of Basic and Applied Science  
International Islamic University, Islamabad



---

## Final Approval

It is certified that the work presented in this thesis entitled "Spin dependent tunneling in spintronics nanomaterials" by Faizan Ahmed, registration No.123-FBAS/MSPHY/F12 fulfills the requirement for the award of degree of MS Physics from Department of Physics, International Islamic University, Islamabad, Pakistan.

### Viva Voce Committee



Chairman \_\_\_\_\_  
(Department of Physics)

Supervisor \_\_\_\_\_

External Examiner \_\_\_\_\_

Internal Examiner \_\_\_\_\_

---

بِسْمِ اللَّهِ الرَّحْمَنِ الرَّحِيمِ

---

***DEDICATED***  
***To***  
***My beloved***  
***Grandparents***  
***Parents***  
***and***  
***My***  
***Respected Teachers***

---

## Declaration

I, **Faizan Ahmed** (Registration # 123-FBAS/MSPHY/F12), student of MS Physics (session 2012-2014), hereby declare that the work presented in this thesis entitled “**Spin dependent tunneling in Spintronic nanostructures**” of MS degree in Physics from International Islamic University Islamabad, is my own work and has not been published or submitted as research work or thesis in any form in any other university or institute in Pakistan or aboard.



**Faizan Ahmed**

(123-FBAS/MSPHY/F-12)

Dated: 7-7-2015

---

## Forwarding Sheet by Research Supervisor

The thesis entitled “Spin dependent tunneling in spintronic nanostructures” submitted by **Faizan Ahmed** (Registration # 123-FBAS/MSPHY/F12) of MS (Physics) has been completed under my guidance and supervision. I am satisfied with the quality of his research work and allow him to submit this thesis for further process to graduate with Master of Science degree from Department of Physics, as per IIU Islamabad rules and regulations.

**Dr. Naeem Ahmed**

Assistant Professor (TTS)  
Department of Physics,  
International Islamic University,  
Islamabad.

Dated: 7-7-2015



---

## **Acknowledgment**

First, I owe my deepest gratitude to **Allah** Almighty for all of HIS countless blessings. I offer my humblest words of thanks to HIS most noble messenger **Hazrat Muhammad (P.B.U.H)**, who is forever, a torch of guidance and knowledge for all humanity. By virtue of his blessings today I am able to carry out our research work and present it.

I would like to acknowledge the worth mentioning supervision of **Dr. Naeem Ahmed** who guided me and supported me during my whole research work. Moreover, their supervision enabled me to develop an understanding of the field. Without their sincere efforts I was unable to complete this hard task of my life. Really I am thankful to **Dr. Naeem Ahmed** for their inspiration and encouragement in every field of life especially in education and teaching. May **Almighty Allah** bless them with long life, health, happiness and knowledge.

Moreover, I would like to express my sincere thanks to all the faculty members of Department of Physics IIU Islamabad especially to **Dr. Waqar Adil Syed** (Chairman). I would also like to thank all other faculty members of my university for their sincere appreciation, comments and suggestions. I express my thanks to all staff of Physics Department, IIU, for their various services. I shall express my heartiest thanks to all my senior research colleagues and my class fellows, without their guidance it was not possible to complete this work.

I also want to pay special thanks to Professor Han Xiufeng of Institute of Physics (IOP), Beijing China for his untiring efforts to provide me sample preparation facility in clean room.

I especially want to acknowledge efforts and prayers of my grandparents, parents, brother and sisters for their love, care and support in my life, which has been directly encouraging me for my study. My parent's prayers are always a source of my success. Allah may bless my parents, teachers and family with long life, health and happiness.

**Faizan Ahmed**

---

## Table of Contents

<b>Chapter No 01</b>	<b>Introduction</b>	
1.1	Nanomagnetism	15
1.2	Fundamental of Magnetism	16
1.3	Classification of magnetic materials	16
	1.3.1 Diamagnetic materials	17
	1.3.2 Paramagnetic materials	17
	1.3.3 Ferromagnetic materials	18
	1.3.4 Anti ferromagnetic materials	18
1.4	Spintronics	19
1.5	Spin up/down band structure.	19
1.6	Spin diffusion length:	20
1.7	Magnetoresistance and it various types:	20
	1.7.1 Ordinary magnetoresistance effect (OMR).	21
	1.7.2 Giant magnetoresistance effect (GMR).	21
	1.7.3 Tunnel magnetoresistance effect (TMR).	21
	1.7.4 Colossal magnetoresistance effect (CMR).	22
1.8	Inter layer exchange coupling	22
1.9	Spin dependent transport	23
1.10	Magnetic tunnel junction (MTJ's).	23
1.11	Half-metallic materials	25
1.12	The exchange bias effect	25
1.13	Spin Valves	26
1.14	Spin Polarization	27
1.15	Simmon`s model	27
1.16	Application of Spintronics	28
	1.16 .1 TMR read head based on MTJ's	28
	1.16 .2 Magnetic sensors	28
	1.16 .3 Magnetic Random Access Memory (MRAM)	29
	1.16 .4 MRAM Field Switching	29
1.17	Motivation	29
1.18	Literature Review	30
<b>Chapter No 02</b>	<b>Synthesis of Nanomaterial</b>	
2.1	Top –down vs Bottom up	32

2.2	Sputtering	32
2.3	DC diode sputtering	32
2.4	RF diode sputtering	33
2.5	Magnetron sputtering	34
2.6	UV Lithography	35
2.7	Ion-beam etching	36
2.8	Vibrating Sample Magnetometer (VSM)	37

### **Chapter No 03                      Experimental Techniques**

3.1	Optical microscope	38
3.2	Scanning Electron Microscopy	38
3.3	Two Point Probe Method	40
	3.3.1 Problems of two probe method	40
3.4	Four point probe method	41
	3.4.1 Measuring resistance of MTJ by Four point Probe method	42

### **Chapter NO 04                      Results and Discussions**

4.1	CoFeB /Al-O/ CoFeB Single barrier magnetic tunnel junctions	43
4.2	Fabrication Of Magnetic Tunnel Junction	44
	4.2.1 Step 1: Fabrication of bottom electrode	44
	4.2.2 Step 2: Fabrication of tunnel junction	45
	4.2.3 Step 3: Fabrication of Top Electrode	46
4.3	Transport Properties of CoFeB/Al-O/FeB	46
	4.3.1 TMR Ratio in AlO <sub>2</sub> Based Magnetic Tunnel Junction	47
	4.3.2 Magnetic Field Annealing Effects in CoFeB/Al-O/CoFeB MTJ	47
4.4	I-V Characteristic Curve	48
4.5	References	51

---

## List of Figures

### Chapter 1

Fig. 1.1: (a) Zero dimensional [2], (b) 1-dimensional [3], (c) 2-dimensional [1] materials.	15
Fig.1.2: Periodic table of magnetic materials.	17
Fig.1.3: Diamagnetic materials when (a) no field is applied (b) field is applied (C) field is removed.	17
Fig.1.4: Paramagnetic materials when (a) no magnetic field (b) applied magnetic field	18
Fig 1.5: Ferromagnetic material when (a) no magnetic field (b) magnetic field.	18
Fig 1.6: Alignment of magnetic domains in anti-ferromagnetic material.	19
Fig 1.7: Diagram of filled band structure for metals (left) and Ferromagnets (right).	20
Fig 1.8: Diagram show states of GMR (a)High resistance (b) Low resistance	22
Fig 1.9: (a) Basic MTJ structure.	23
Fig 1.9: (b) MTJ structure with AFM pinned layer.	24
Fig 1.9: (c) MTJ structure with SAF and AFM pinned layer	24
Fig 1.9: (d) MTJ structure with SAF pinned Layer	25
Fig 1.10: Exchange biased effect after field cooling.	26
Fig 1.11: Working of spin valve	26
Fig 1.12: Demonstrate J1 and J2 peaks at T=300K.	27
Fig 1.13: Diagram of Bio sensor MTJ.	29

### Chapter 2

Fig.2.1:Structure of basic DC diode sputtering system.	33
Fig 2.2: Basic structure of RF sputtering system.	34
Fig.2.3:Showing Basic components of Magnetron sputtering system.	35
Fig. 2.4: Diagram representation of three stages involved in photolithography.	36
Fig.2.5: Structure of VSM	37

### Chapter 3

Fig. 3.4: Schematic diagram of Scanning electron microscope	39
Fig 3.5: Setting of two probe system	40
Fig 3.6: Diagram of four point probe setting.	41
Fig 3.7 : Schematic representation of current in plane tunneling method by four point probe.	42

### Chapter 4

Fig 4.1: Diagram represent multilayer stack of MTJ	43
Fig 4.2: Shows the fabricated bottom electrode.	44
Fig 4.3: Appearance of SiO <sub>2</sub> depositions on the sample	45

---

<b>Fig: 4.4:</b> (a) left shows sample before dipped in acetone. (b) Right shows sample after dipped in acetone	46
<b>Fig: 4.5:</b> Resistance Curve of SBMTJ before MF annealing at room temperature.	47
<b>Fig 4.6:</b> TMR curve at room temperature after MF annealing	48
<b>Fig 4.7:</b> Linear I/V curve of SBMTJ at room temperature for anti-parallel state.	48

---

## List of Tables.

Table 3.1 Images by Optical microscope	38
Table 4.1 Stages of fabrication	45

---

## Abstract

Spintronics is the manipulation of spin degree of freedom rather than charge of electron in the devices. A magnetic tunnel junction (MTJ) is a spin valve type nanostructure in which one insulating layer is sandwiched between two ferromagnetic layers. Magnetic Tunnel Junctions CoFeB(3nm)/AlO(1nm)/CoFeB(4nm) have been prepared by magnetron sputtering system, Ion beam etching and photolithography on SiO<sub>2</sub> substrate in a base pressure of  $P = 10^{-8}$  Torr. The IV curves and Tunneling Magnetoresistance (TMR) are measured at room temperature with the help of four point probe method. It is observed from IV curves that the resistance of the MTJ is  $\sim 115 \Omega$ . The TMR of the MTJ is found to be 24% when a magnetic field of 300 Oe is applied in the plane of MTJ at room temperature. The MTJs were annealed in the magnetic field  $H_{\text{ann}} = 400$  Oe at Temperature  $= 265^\circ\text{C}$  for one hour. It is interestingly observed that TMR increases from 24% to 38%. The increase in TMR is attributed to smoothening of the interface and crystallinity of the ferromagnetic layers. Beside this IV curves are fitted with the Simon's model. The experimental values from the IV curve are fitted well with the model and barrier height is found to be in the range of few eV. This study will be useful to study spin transfer torque and spin-orbit coupling in MTJs for the future applications of Magnetic random access memory (MRAM) which is a non-volatile memory.

# Chapter 1

## Introduction

### 1.1 Nanomagnetism:

Nanomagnetism is the youngest field of research and affected every sphere of human activities through its contribution in the field of medicine, computers, communication and scientific investigations. Nanoscience is the study of preparation, process and properties of objects in the dimension range from 1nm to 100nm. The size of molecules, viruses and many components of integrated circuit lies in 1nm to 100nm range.

In Physics, nanomagnetism is that field of investigation in which magnetic properties and application of materials that have as a minimum one dimension in the nanoscope range are considered. Those materials that hold nano-particles, multi-layer, thin-films and other structures in the nanometer scale can express as nano structured materials.

The feature that enhances magnetic properties of the nanomaterials are characteristic length, broken translation symmetry, density of electronic state curve shape, proportion of surface atoms and physical properties of substrate and capping layer material in the case of thin-film/multilayer. The properties of material changes drastically when the size of material decreases to nano meter range and its surface area to volume ratio increases greatly. Magnetic memory of nanomaterials depend upon its size [1]. In figure 1.1 SEM images of (a) Zero-dimension (b) 1-dimension nano-particles (c) 2-dimension nano-particles are shown.

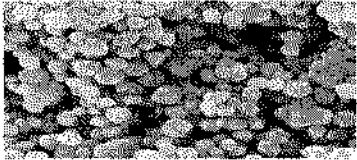
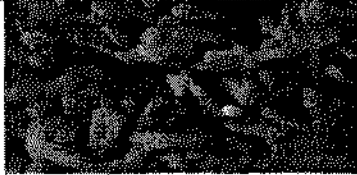

Material with zero-dimension [5]	 (a)
Material with 1-dimension [6]	 (b)
Material with 2-dimension [7].	 (c)

Fig. 1.1: (a) Zero dimensional [2], (b) 1-dimensional [3], (c) 2-dimensional [1] materials.

Nanomagnetism has many daily life applications extended from geology to magnetic recording, from ferro-fluids applied in loudspeaker to nano-particles used in medicine.



Among all these applications nanomagnetism has made advancement in the field of magnetic recording and reached to higher and higher storage densities.[2-3]

The applications that rely on the 'spin degree of freedom' of charge in an electric current within the magnetic material are also uses thin-films, multilayers and other structures with nanomateric dimensions.

### 1.2 Fundamental of Magnetism

A material experiences a force of attraction or repulsion when placed in an external applied magnetic field due to the magnetic moment in material. Bohr's model explains how magnetism can occur due to the motion of electron in an atom. An orbiting electron around a nucleus generates a magnetic moment

$$\mu = i A \quad (1.1)$$

here  $i = dq/dt$  and  $A$  is oriented area enclosed by the loop.

$$\mu = (dq/dt) \pi r^2 \quad (1.2)$$

for electron in circular orbital with speed 'v'

$$\mu = (ev/2\pi r) \pi r^2 \quad (1.3)$$

$$\mu = (e/2m) 2mv \quad (1.4)$$

here  $L = 2mv$  is the angular momentum

$$\mu = (e/2m_e) L \quad (1.5)$$

Finally in equation (1.5) we get basic relation called gyro-magnetic, that accounts for atomic orbital magnetism. When the large number of atomic scale magnetic moments are aligned in the material it is called magnetization  $M$  and can be calculated as the magnetic moment per unit volume.

### 1.3 Classification of magnetic materials

There are five different classes of magnetic materials classified on the basis of magnetic behavior of magnet and there magnetic properties.

- ❖ Diamagnetism in Diamagnet
- ❖ Paramagnetism in Paramagnet
- ❖ Ferromagnetism in Ferromagnet
- ❖ Anti-ferromagnetism
- ❖ Ferrimagnetism

Figure 1.2 Show the periodic table of magnetic materials

1 H	<input type="checkbox"/> Ferromagnetic <input type="checkbox"/> Antiferromagnetic																2 He													
3 Li	4 Be	<input type="checkbox"/> Paramagnetic <input type="checkbox"/> Diamagnetic										5 B	6 C	7 N	8 O	9 F	10 Ne													
11 Na	12 Mg											13 Al	14 Si	15 P	16 S	17 Cl	18 Ar													
19 K	20 Ca	21 Sc	22 Ti	23 V	24 Cr	25 Mn	26 Fe	27 Co	28 Ni	29 Cu	30 Zn	31 Ga	32 Ge	33 As	34 Se	35 Br	36 Kr													
37 Rb	38 Sr	39 Y	40 Zr	41 Nb	42 Mo	43 Tc	44 Ru	45 Rh	46 Pd	47 Ag	48 Cd	49 In	50 Sn	51 Sb	52 Te	53 I	54 Xe													
55 Cs	56 Ba	57 La	72 Hf	73 Ta	74 W	75 Re	76 Os	77 Ir	78 Pt	79 Au	80 Hg	81 Tl	82 Pb	83 Bi	84 Po	85 At	86 Rn													
87 Fr	88 Ra	89 Ac																												
		<table border="1"> <tr> <td>59 Ce</td> <td>60 Pr</td> <td>61 Nd</td> <td>62 Pm</td> <td>63 Sm</td> <td>64 Eu</td> <td>65 Gd</td> <td>66 Tb</td> <td>67 Dy</td> <td>68 Ho</td> <td>69 Er</td> <td>70 Tm</td> <td>71 Lu</td> </tr> </table>															59 Ce	60 Pr	61 Nd	62 Pm	63 Sm	64 Eu	65 Gd	66 Tb	67 Dy	68 Ho	69 Er	70 Tm	71 Lu	
59 Ce	60 Pr	61 Nd	62 Pm	63 Sm	64 Eu	65 Gd	66 Tb	67 Dy	68 Ho	69 Er	70 Tm	71 Lu																		

Fig.1.2: Periodic table of magnetic materials.

### a) Diamagnetic material

Materials in which no unpaired electrons present and all the orbitals are filled due to which they have no net magnetic moments. However, when they are placed in the external magnetic field  $H$  all the magnetic moments are aligned in opposite direction to the applied magnetic field direction. These materials show temporary magnetization because they losses its magnetization when external magnetic field is removed and produces negative magnetization as a result, the susceptibility  $\chi_m$  of diamagnetic material is  $< 0$  (order of  $-10^{-5}$ ) [4-5].

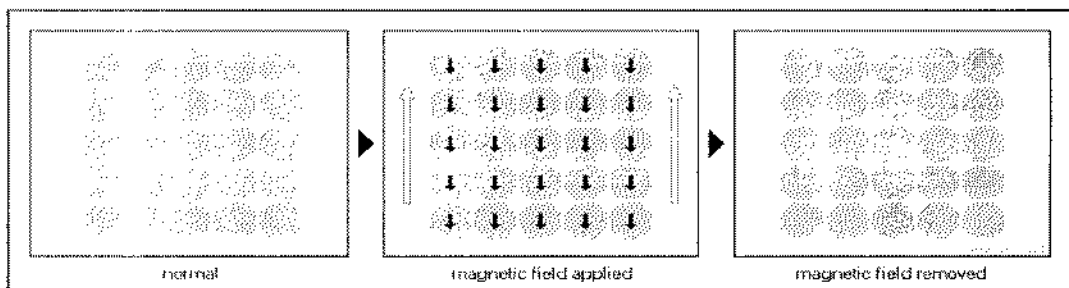


Fig.1.3: Diamagnetic materials when (a) no field is applied (b) field is applied (C) field is removed.

### b) Paramagnetic materials

These materials have partially filled orbitals resulting unpaired electrons which cause magnetic moment but with disorder orientation. In Fig 1.4 (a) when  $H=0$  all magnetic moments are randomly oriented and in fig 1.4 (b) When magnetic field  $H$  is applied all the magnetic moments aligned in the direction of magnetic field and a net magnetization  $M=M_0$  occurs with positive susceptibility.

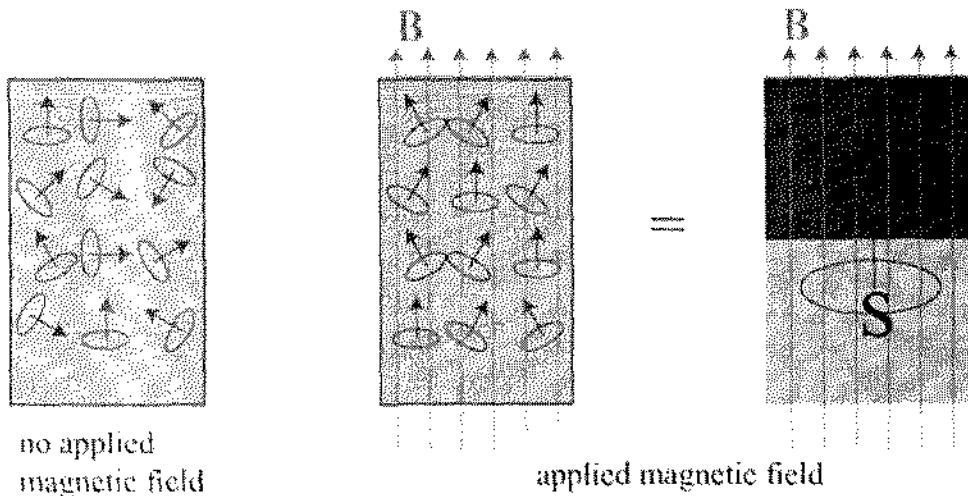


Fig.1.4: Paramagnetic materials when (a) no magnetic field (b) applied magnetic field

**c) Ferromagnetic material**

The magnetic moments of atom or ions are parallel in ferromagnetic materials and also permanently self-aligned in the direction of applied magnetic field even when the magnetic field is removed. These magnetic moments are originated by the contribution of electron spin and orbital magnetic moment. For example Co, Fe, Ni etc are ferromagnetic materials and their magnetic susceptibility is very high mostly in the range of  $10^6$ . [4]

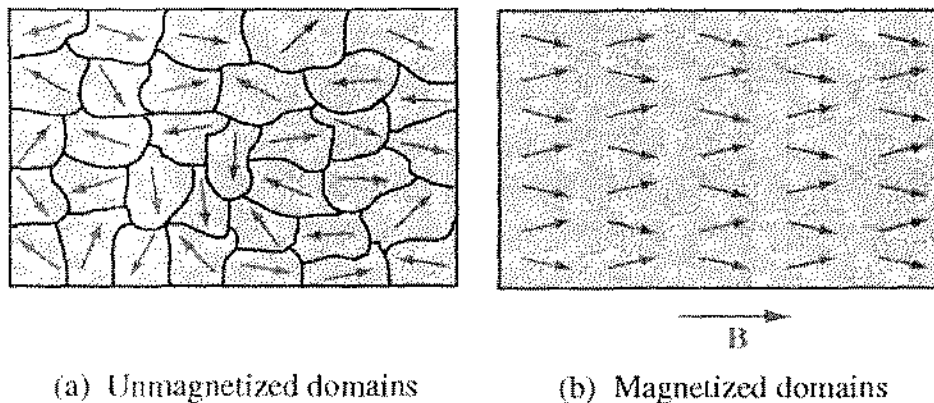


Fig.1.5: Ferromagnetic material when (a) no magnetic field (b) magnetic field.

**d) Anti ferromagnetic material**

In anti-ferromagnetic materials the interaction of magnetic moments between adjacent moments tends to align them anti-parallel. In figure 1.6 it is illustrated that one set of magnetic ions is spontaneously magnetized below Neel temperature and other set is spontaneously magnetized at the same amount but in opposite direction. As a result there is no net spontaneous magnetization take place. Anti-ferromagnetic materials behave as

paramagnet at fixed temperature in the presence of external magnetic field and the susceptibility is positive and small.[6]

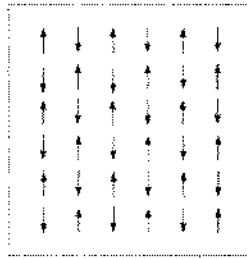


Fig.1.6: Alignment of magnetic domains in anti-ferromagnetic material.

#### 1.4 SPINTRONICS:

Spintronics is the branch of physics that deals with the electron spin degree of freedom for storage and transfer of data. Spintronic has attracted the researcher from the field of nano-electronics and material science after the discovery of GMR effect in late 80's and earlier 90's by two groups, Peter Gruenberg Group and Albert Fert's Group [7-8]. After this discovery the storage capacity of magnetic material has increased dramatically in recent years. Now a day's physicists are focusing on the spin of electron rather than charge to create remarkable spintronic devices which will be compact, robust and more versatile. Spintronics is the new and wide field in which magnetic technology and semi-conductor technology is the base and it is supported by quantum mechanics.

The quantum mechanical property of electron called the intrinsic angular momentum named as 'electron spin'. There are two magnetic moments associated with an electron one orbital angular momentum ( $\mu_B = eh/2m_e$ ) and other intrinsic angular momentum 'spin' ( $\mu_z = g (eh/2m_e)m_s$ ) here  $g$  is the gyro magnetic ratio, its value is 2.002 for electron spin,  $m_s$  is  $+\frac{1}{2}$  and  $-\frac{1}{2}$ . In 1988 it was demonstrated that current flowing from ferromagnetic material into any metal it does not change its spin orientation atleast for a distance equal to interatomic spacing. After this discovery it was investigated in many spintronic devices that spin with its associated magnetic moment can be transported just as charge hence magnetization can be transferred from one material to another.

#### 1.5 Spin up/down band structure.

In metals the number of up-spin is equal to down-spin electrons at the Fermi level in partially filled s-band. But in ferromagnets the narrow d-band shifted by an amount  $2\mu_B E_E$ , here  $E_E$  is the internal exchange field that is represented by exchange interaction  $J_E = 3k_B T_C / 2zS(S+1)$ , this results the total number of majority up-spin electrons exceeds the total number of minority down-spin electrons as shown in figure 1.7. the density per unit

energy of up-spin state can be changed to down-spin at the Fermi level due to the ferromagnetic transition temperature. In tunnel valve this basic property of ferromagnet is used and applicable in magnetic field sensor used in Magnetic Disk Drives [9].

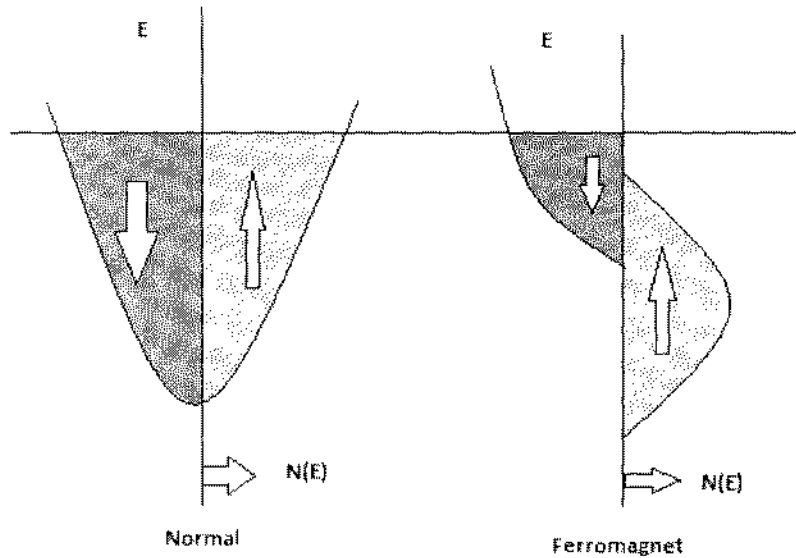


Fig 1.7: Diagram of filled band structure for Metals (left) and Ferromagnets (right).

Since DOS are split corresponding to two different spins of electrons at the Fermi level due to ferromagnetic exchange energy stated by Mott's model, the conduction in metals can also be studied by considering the electron configuration and their magnetic properties. [10-11].

### 1.6 Spin diffusion length:

The up-spins converted to down-spins due to the spin flip processes. The length scale which describe how far from the interface the spin accumulation decays exponentially is mathematically given below in equation 1.6.

$$\lambda_{sd} = \sqrt{\lambda v \tau_{\uparrow\downarrow}/3} \quad (1.6)$$

Where is ' $\tau_{\uparrow\downarrow}$ ' spin flip time,  $v$  Fermi velocity,  $\lambda$  the mean free path and  $\lambda_{sd}$  spin diffusion length.

Introducing impurities in silver helps to reduce mean free path and also drops the spin flip time which cause decrease in spin diffusion length due to more spin orbit scattering.[12]

### 1.7 Magnetoresistance and Types:

Magnetoresistance is the phenomenon in which a material changes its electrical resistance when the magnetic field is applied on it. It is measured quantitatively by a formula,

---

where  $R_H$  is resistance of a sample with magnetic field and  $R_0$  is the resistance without magnetic field.

$$MR = (R_H - R_0) / R_H \quad (1.7)$$

In modern technology, the magnetic field sensors are based on the effects called Giant magnetoresistance 'GMR' or tunnel magnetoresistance 'TMR'. These effects are usually observed in nanomaterials, if conducting layers are smaller than the mean free path  $\lambda_{sf}$  of an electron so that to change its spin orientation (spin flip). In magnetoresistance situation a longer mean free path and spin flip is very important behavior.

There are different types of magnetoresistance effects depending upon following mechanisms.

**i) Ordinary magnetoresistance effect (OMR).**

This effect is only observed and measured in metals because metals have large mean free path in the absence of magnetic field. When a magnetic field is applied charge carriers reduces its mean free path by revolving in the orbits, which cause a change in electrical receptivity of metal. This change reaches to few percent in magnetic field.

**ii) Giant magnetoresistance effect (GMR).**

GMR effect is observed in multilayer ferromagnetic layers separated by nonmagnetic or anti-ferromagnetic layer [13-16]. GMR describes a huge change of electrical resistance in applied magnetic field. This electrical resistance depends on the relative movement (orientation) of magnetic moments in magnetic and nonmagnetic layers. If both layers are in anti-parallel states then it shows maximum electrical resistance and if both layers are in parallel states then it shows minimum electrical resistance. These phenomena give an idea of non volatile magneto resistive random access memory devices [17]. To understand GMR it is important to know two basic concepts, first interlayer exchange coupling and second spin dependent transport.

**iii) Tunnel magnetoresistance effect (TMR).**

Tunnel valve is composed of metal-insulator-metal junction; consist of soft magnet NiFe, an non-conducting  $Al_2O_3$  or MgO tunnel barrier and Co as a hard magnet. Tunnel magneto resistance effect is usually observed in magnetic tunnel junctions (MTJ's) device. The tunnel current preserves the direction of spin from one electrode to the other, according to the rule that down-spin state at the opposite electrode only accepts the down-spin electrons and similarly for up-spin electrons. The tunneling current is appropriately observed across the tunneling barrier and thus tunneling resistance (TMR) is calculated by equation (1.8).

$$\text{TMR} = \{(R_{ap} - R_p) \div R_p\} \times 100 \% \quad (1.8)$$

$R_{ap}$  and  $R_p$  is the resistances when the two magnet layers are anti parallel and parallel to each other respectively. The resistance varies exponentially with the insulating barrier thickness [19-20]. Tunneling current is measured that is proportional to the product of initial DOS at Fermi level and final DOS at opposite electrode. TMR can also be calculated by formula (1.9).

$$\text{TMR} = 2P_1P_2 / (1 - P_1P_2) \quad (1.9)$$

iv) **Colossal magnetoresistance effect (CMR).**

This CMR effect is observed by Jin et al, when large magnetic field is applied on manganese-based perovskite oxides at Curie temperature [21-23]. The change of electrical resistance is very high in order of magnitude. This change needs large field in few Tesla so therefore CMR has no practical applications so far.

**1.8 Inter layer exchange coupling:**

It governs the relative movement (orientation) in the magnetic material called magnetization, it is either coupled ferro-magnetically or anti-ferromagnetically by adjusting thickness of non-magnetic layer. For small inter spacing layer the magnetic layers couple ferromagnetically and for large inter spacing layer the magnetic layer couple anti-ferromagnetically. GMR occurs if the spacer layer is adjusted such that the magnetic layers couple anti-ferromagnetically at zero magnetic field as demonstrated in figure 1.8(a) and interlayer exchange coupling is negative, producing high resistance. Similarly by applying magnetic field the orientation of magnetic layers aligned parallel as demonstrated in figure 1.8 (b) and produces low resistance.

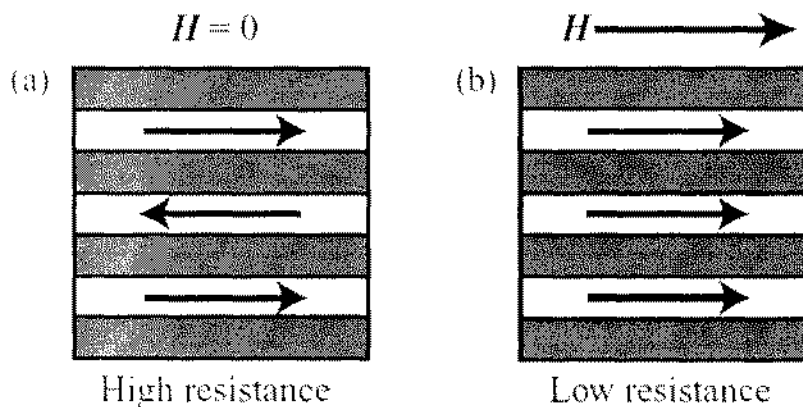


Fig 1.8: Diagram show states of GMR (a)High resistance (b) Low resistance.

### 1.9 Spin dependent transport:

In fig 1.8(a) anti-parallel orientation has high resistance because the spin-up electrons are scattered by spin down magnetized layer and similarly the spin-down electrons are scattered by spin up magnetized layer. But in parallel alignment only one spin type can pass through the system and other spin type is strongly scattered resulting in less resistance.

The GMR effect is used in reading and writing magnetic data in the form of 0 and 1 binary data bits. 0 stands for low resistance and 1 stands for high resistance. This technique is used in magneto resistive random access memories MRAM memory cells [18].

### 1.10 Magnetic tunnel junction (MTJs):

MTJ's composed of thin insulating barrier layer sandwich between two ferromagnetic layers [23-27]. The magnetic coercivities of two layers are different so that's why the switching fields of two FM layers are different. The layer with low coercivity is called free layer and other with high coercivity is called pinned layer or fixed layer.

For the conservation of spin of electrons during tunneling process the insulating layer is chosen smooth and thin. It also help to make MTJ's more responsive. Different types of MTJ's are shown below.

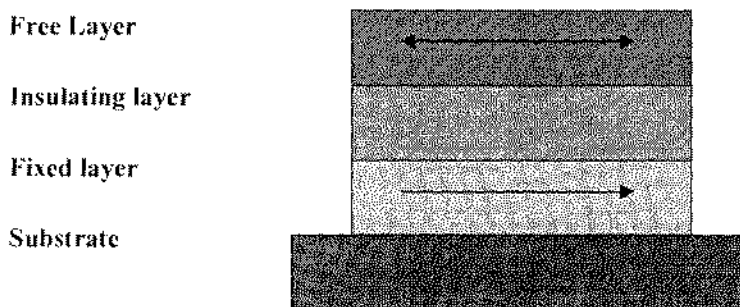


Fig 1.9: (a) Basic MTJ structure.

In fig 1.9(a) the basic MTJ structure is shown. It is used as a memory as long as the coercivity of the pinned layer is higher than the coercivity of the free layer. If the orientation of free layer is changed by applying low field than this would give the switching operation of memory. But this structure has some limitations that this low field activity might cause permanent orientation of small domains in the pinned layer, which reduces the efficiency of the device. [28]



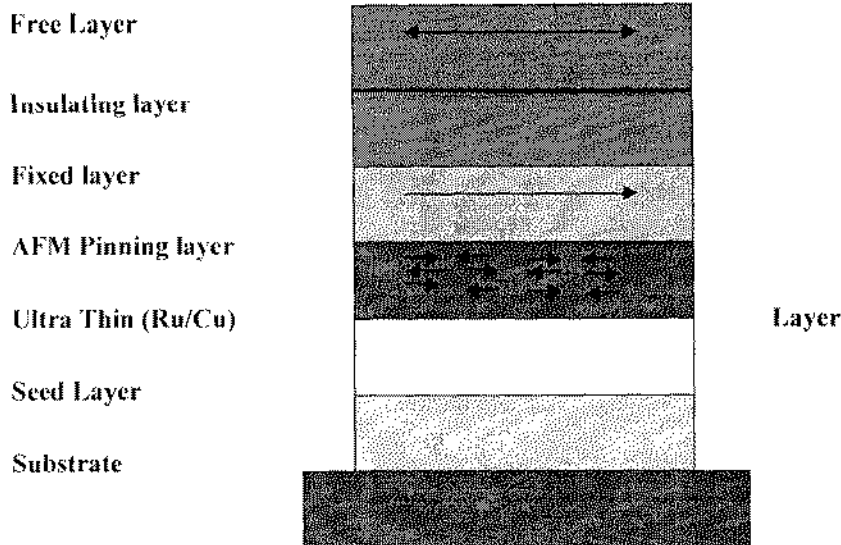


Fig 1.9: (b) MTJ structure with AFM pinned layer

In fig 1.9(b) anti-ferromagnetic layer is coupled with pinned layer to avoid the permanent orientation of domains in the pinned layer by exchange couple effect[29]. To make this exchange coupling effect more effective the interface should be kept very smooth. The limitation of these type of structure is that there exists non-zero magnetic bias on the free layer which would affect the operation of device in the absence of magnetic field.

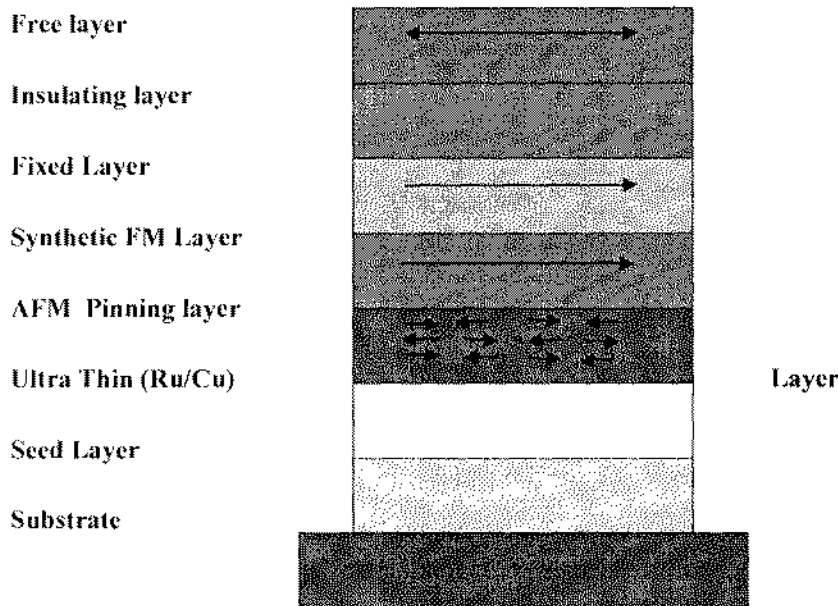


Fig 1.9:(c) MTJ structure with SAF and AFM pinned layer

In fig 1.9(c) Synthetic Antiferromagnetic(SAF) structure is shown which is composed of CoFe/Ru/CoFe with thickness of Ru adjusted to produce pinned layer with non magnetic bias and exchange couples the moment of the two ferromagnetic layers in opposite

directions. The critical thickness found to be  $7-9\text{\AA}$ . The limitations of these type of structure is that it shows unstable behaviour at high annealing temperature[30].

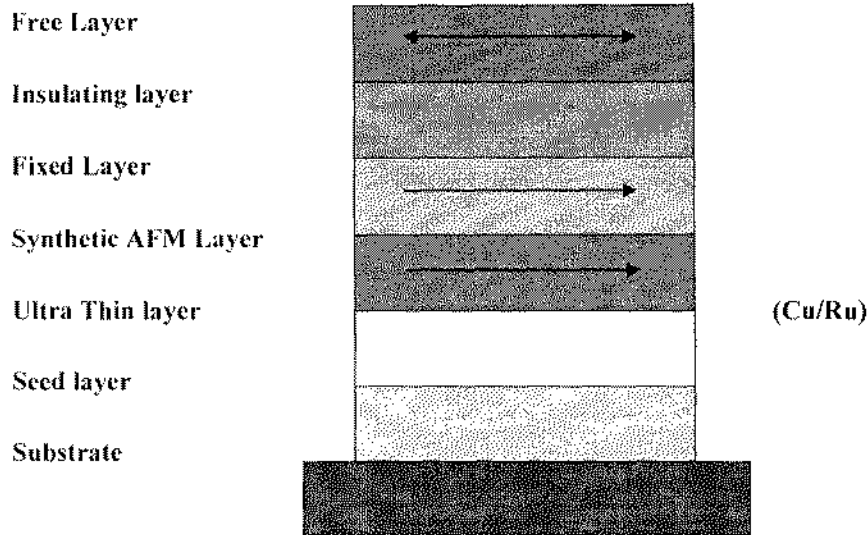


Fig 1.9: (d) MTJ structure with SAF pinned Layer

In fig 1.9(d) the SAF type structure is shown but without exchange biasing by AFM layer. This structure helps to avoid the limitation present due to the AF layer.[31-33].

### 1.11 Half-metallic materials:

Half-metallic materials are materials that are metallic for one spin polarized electrons and insulator for other spin electrons, it mean only one type of electrons are available for conduction. In half-metallic ferro-magnets there exist an energy gap for electrons of one spin direction like up-spin electron between valence bands and conduction bands for the electrons of other spin direction like down-spin electron exist continuous bands, so for that its shows semi-conducting behavior if the minority electrons (spins anti-parallel to magnetization), whereas it can also show metallic behavior if the majority electrons (spins parallel to magnetization). As a result, the conduction electrons are completely spin polarized at the Fermi level. This class of materials was discovered by De Groot *et al.* [34].

### 1.12 The exchange bias effect:

Exchange bias is observed in ferromagnetic/anti-ferromagnetic interface, when cooled in the presence of magnetic field through Neel temperature of anti-ferromagnetic shown in figure 1.10. In this case the Curie temperature of the ferromagnetic material is considered to be above the Neel temperature. [35-38].

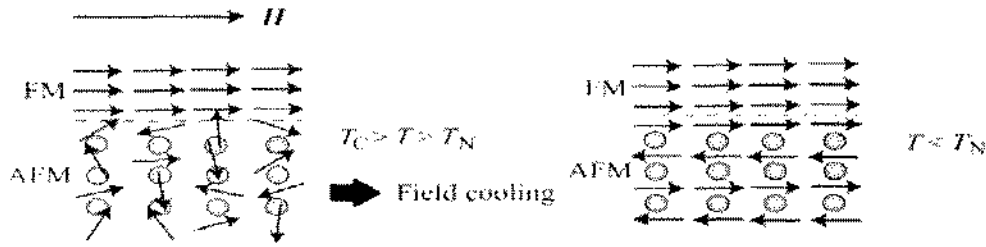


Fig 1.10: Exchange biased effect after field cooling.

The EB effect is also observed in spin valves with one pinned and one free FM layer which are implanted in devices such as readout sensors, storage media and magnetic random access memory (MRAM). The exchange bias (EB) effect has two characteristics firstly when magnetic field is applied it cause magnetic coupling across the interfaces between ferromagnetic and anti-ferromagnetic layers due which hysteresis loop shifts either towards positive or negative axes depending on the direction of applied field [39, 40].Second an increase in coercivity and a wider hysteresis loop.

### 1.13 Spin Valves:

Spin valve is composed of two FM layer separated by a non magnetic layer called spacer layer as illustrated in figure 1.11. The magnetization of one FM layer is free to change the orientation which is pinned to the other FM layer by exchange biased coupling with adjacent anti-ferromagnetic 'AFM' layer [41].When the field is changed between positive and negative value, the magnetization of two FM layers also changes from anti-parallel to parallel state. During this change the magnetoresistance change from high to low value. This phenomenon corresponds to switching of free layer.

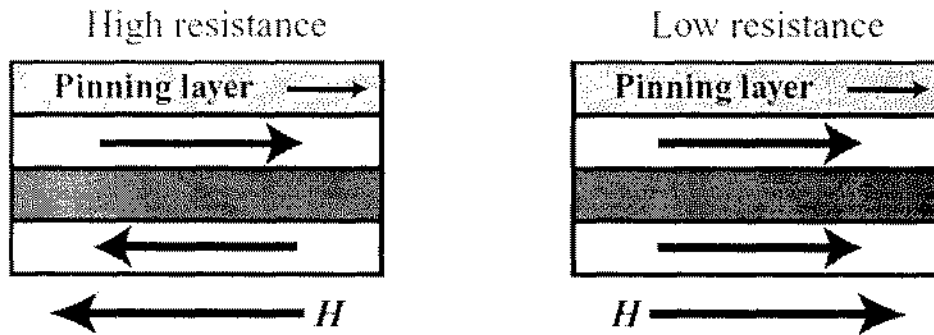


Fig 1.11: Working of spin valve

The interesting features of Spin valve is that it shows high magnetoresistance sensitivity of the order of ten of percent at low magnetic field of the order of tens of oersteds.

### 1.14 Spin polarization:

The process in which one spin direction is allowed during transport process because of the energy gap for other spin direction usually for minority spin bands at Fermi level and result in spin polarization. This effect is observed in half metallic ferromagnets and is used as ferromagnetic electrodes in spintronic devices. In MTJ's when two ferromagnetic layers are aligned in anti-parallel state then the magnetization of electrodes in applied magnetic field take part and the electrons will spin polarized during the transport process. According to Julliere's model the spin polarization is used to calculate TMR value using formula as explained below.[19-20]

$$TMR = 2P_1P_2 / (1 - P_1P_2) \quad (1.10)$$

$P_1$  and  $P_2$  is the spin polarization of ferromagnetic electrodes and there values depends on the density of states at Fermi level for minority and majority spins.

### 1.15 Simmon's model:

In simmon's model the J-V characteristic curve at varying temperature for tunneling junction is expressed in generalized theory. This theory is applied to two junctions one symmetric and other Asymmetric. In symmetric junction the parabolic curve increase with increase in temperature and voltage bias to a certain peak percentage value and decrease abruptly afterward. This critical voltage bias at which thermal percentage of current density is maximum is proportional to interfacial barrier height.

Similarly for Asymmetric junction the theory derives two peaks values of percentage current density J and depends upon the polarity of voltage biased and electrode-insulator interfacial barrier heights  $\phi_1$  and  $\phi_2$ . Figure 1.12 demonstrate J-V curves.

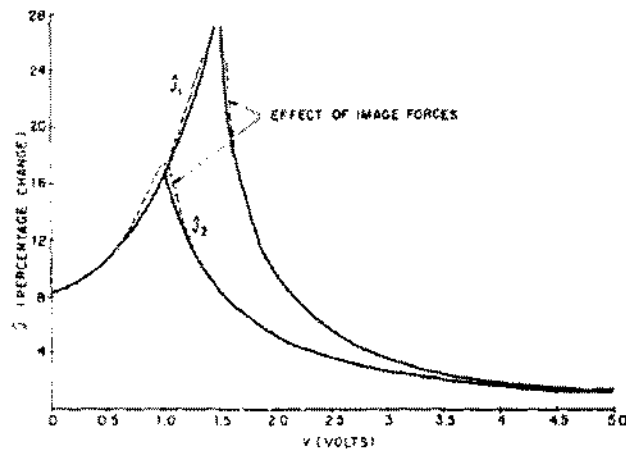


Fig 1.12: Demonstrate J1 and J2 peaks at T=300K.

---

Here in this model the thickness to insulating layer is adjusted 20 and concluded  $\phi_1 = 1V$  which is the small Asymmetric interfacial barrier height and  $\phi_2 = 1.5V$  which is the large Asymmetric interfacial barrier height.

#### **1.16 Application of Spintronics:**

- Read/Write data in Hard disk drives
- Bio sensors.
- Micro electromechanical system
- Magneto resistive random-access memory
- Nano magnetic oscillator
- Molecular Electromechanical devices
- Molecular optoelectronics

MTJ's is used in device application for this it can describe the antiquity of spintronics or the antiquity of magneto resistance at room temperature. Now a days read heads of HDDs with MR ratios of 5% to 15% are GMR based spin valves devices at room temperature, Also AI-O based MTJ's are used in HDD read heads and MRAM cells due to its high MR ratios of 20% to 70% at room temperature.

##### **1.16 .1 TMR read head based on MTJ's:**

For spintronic devices, MTJ's are consistent with the mass manufacturing process due to their Gaint TMR effect. By sputtering deposition method at room temperature it can be fabricated on pinned layer structure after performing post annealing. To meet challenges of industrial applications, the requirement of standard MTJ's must have MR ratios with low bias voltages.

##### **1.16 .2 Magnetic sensors:**

MTJ's have many advantages such as

- i) High TMR ratio
- ii) Small size
- iii) Low cost
- iv) Lab-on-chip compatibility

According to these benefits they are reflected as an ideal sensor element for biosensors and biochips [42]. The sensing stage of MTJ's together with magnetic nano particles (MNP) has been effectively applied for detecting protein binding and DNA hybridization [43]. Figure 1.13 describes the bio sensor MTJ.

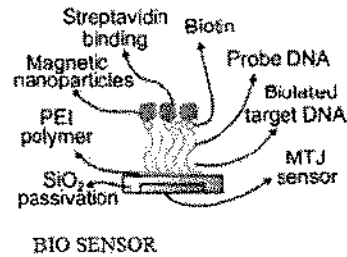


Fig 1.13: Diagram of Bio sensor MTJ.

### 1.16.3 Magnetic Random Access Memory (MRAM):

Resistance differences of MTJ's can be used to store information in electronic form 0 & 1 for parallel and anti-parallel state respectively. As a result, MTJ's based on TMR effect can be used to fabricate novel MRAM with properties like non-volatility, processing quickly, transferring, low energy cost and storage into one chip.

### 1.16.4 MRAM Field Switching:

Conventional MRAM uses the magnetic fields produced by currents to switch the memory states (0 to 1) or (1 to 0) of the MTJ memory cell. In write process, current generate magnetic field while passing through programming lines. The combine effect of two magnetic fields by top and bottom lines are used to program the bit.

### 1.17 Motivation:

As spintronics is the new field of research in Physics and applications based on the intrinsic property called spin. In past few years scientist worked on MgO or AlO based MTJ's and their aim were to measure high TMR values, so they succeed to measured maximum GMR and TMR value at low Temperature, which was very helpful in practical applications like spintronic devices but our main focus in this research is on AlO based MTJ's and measuring TMR value at room temperature which has many future applications. These MTJ's are used in magnetic sensors, read/write head and data storage devices.

My motivation in this research is to fabricate Single barrier AlO based Magneto tunnel junction and measure the characteristics like I-V curve, TMR ratio before and after magnetic annealing, structure morphology of multilayer by XRD and SEM techniques.

Accepted for No. 19635

---

### 1.18 Literature Review:

In spintronics, the Al-O and Mg-O based magnetic tunnel junction (MTJ) has open research advancement because of its three main features

- i) Physical effects like spin transfer torque, spin-caloric effect, coulomb blockade magneto resistance effect etc.
- ii) Physical properties like GMR, TMR etc.
- iii) Device applications like spin logic devices, MRAM, read heads, magnetic sensors etc.

First time the TMR effect was introduced in 1975 by Julliere *et al*, reported TMR ratio 14% at 4.2K in Fe/Ge-O/Co MTJ. Here Fe and Co is ferromagnet and Ge-O is insulating layer. In their work they defined TMR ratio by a formula.

$$\text{TMR} = (G_P - G_{AP}) / G_{AP} = 2 P_1 P_2 / (1 - P_1 P_2)$$

Where  $G_P$  and  $G_{AP}$  are the conductances and  $P_1, P_2$  are the spin polarization of ferromagnetic electrodes.

By optimizing the ferromagnetic electrodes and changing the conditions of fabrication many researchers reported significant increase in TMR ratio. In 1995 Miyazaki et al and Moodera et al obtained 18% TMR ratio at room temperature by fabricating MTJ with tunnel barrier of amorphous aluminium oxide and 3d ferromagnetic electrodes.

The objective to achieve maximum TMR ratio the researcher has predicted theoretically that it can be increased by tunneling of coherent electrons. Parkin et al in 2004 reported 180% TMR ratio at room temperature by fabricating MgO based MTJ (Fe/MgO/Fe) using molecular beam epitaxy (MBE).

It has been reported that researcher are interested to increase TMR ratio by fabricating MTJ differently and devoted their efforts for optimizing the structure, ferromagnetic electrodes and barrier layer to achieve the goal.

For practical application like magneto sensitive sensor in 2001 it was predicted that by using crystalline MgO (001) or textured MgO (001) barrier layer, the researcher of that time obtained upto 500% TMR ratio at room temperature in CoFe/MgO/CoFe MTJ. And by following first principal theory they expected 1000% TMR ratio, the reason for that is the momentum, which does not remain conserved in amorphous material during tunneling process because the electrons are scattered inside the barrier and destroys the symmetry of

---

coherent electrons but it is conserved in crystalline materials hence increase the probability of TMR value.

Nozaki *et al* reported property called spin dependent tunneling conductance in fully epitaxial Mg-O pseudo-spin valve type double barrier MTJ deposited by MBE method [ Mg-O (10) seed layer/Fe(50)/Mg-O(2)/Fe(t)/Mg-O(2)/Fe(15) ], researcher varied the Fe middle layer thickness in Nano-scale from 1 to 1.5 nm by quartz oscillator and observed the spin dependent tunneling conductance by varying biased voltage. In their research they also vary the temperature (4.5, 100.RT) and observe spin dependent tunneling conductance as a function of biased voltage and calculated TMR ratio upto 136%.

Miao *et al* reported in 2006 that by depositing Mg inter layer barrier layer varying from 0 to 10 Å and observed change in TMR ratio due to the long diffusion length of Bloch state in Mg. By increasing the thickness above 10Å, resulting a decrease in the TMR ratio due to the partial conversion of Mg into Mg-O layer which in turn break the coherence between barrier and ferromagnetic electrodes.

Maisumoto *et al* in 2009 deposited flat ultra-thin Cr (001) layer just below MgO barrier layer in MTJ ( Fe/Cr/MgO/Fe(001)) and investigated spin dependent transport. It is reported by the researcher that by fabricating such MTJ helps to overcome the scattering process of tunneling electron and increase the TMR ratio. It is determined that the exponential increase in junction resistance with increase in Cr spacer layer.

In 2010 it is reported by Gen *et al* that by optimizing middle free layer structure(Co<sub>40</sub>Fe<sub>40</sub>B<sub>20</sub>) the TMR ratio can be enhanced. So the researchers fabricated MgO based double barrier MTJs by using photolithography and Ar ion milling technique and deduce 130 % TMR ratio annealed at 350C.

Yamamoto *et al* in 2012 reported that by increasing concentration of Mn in Co based heusler alloy (Co<sub>2</sub>Mn $\alpha$ Si) electrode and MgO tunnel barrier the TMR ratio increases to 1135% at 4.K and 236 % at room temperature and biased voltage 1mV by adjusting value of  $\alpha=1.29$  in the fabrication of MTJ layer structure [ MgO buffer (10)/CMS(30)/MgObarrier(2-3)/CMS(4-5)/Ru(0.8)/Co<sub>80</sub>Fe<sub>20</sub>(2)/Ir<sub>22</sub>Mn<sub>78</sub>(10)/ Ru(5nm) ] deposited on MgO substrate.



---

## Chapter 2

### Synthesis of Nanomaterials

In this chapter a brief study of experimental procedures followed during the sample preparation and device fabrication are mentioned. There are two different approaches of fabricating materials. One approach is top-down and second approach is bottom-up.

#### 2.1 Top-down vs Bottom-up:

When the bulk material is machined(crushed) and then modified into desired shapes and products, like manufacturing integrated circuits by the sequence of crystal growth, ion beam etching, lithography etc, than this technique is called top-down approach. For the synthesis of nanomaterials one of the important examples of top-down approach is ball-milling in which macro crystalline structures are broken down without disturbing the integrity of material into nano crystalline structures. In milling process the kinetic energy is supplied to prepare nanostructure metal oxide by chemical reaction between two constituent during crushing.[44-46]

On other hand the technique use in assembling materials from atom or molecules up to form nano fabricated materials is called bottom-up approach. Bottom-up approach is the non- lithographic technique for the synthesis of nanomaterials and has a great potential to overcome the lithographic process in future.PVD, CVD, Sol-gel technology, electro-deposition, laser ablation, epitaxial growth is the example of bottom-up technique.

#### 2.2 Sputtering:

Thin films and multilayers can be deposited on a substrate by sputtering. Sputtering is a physical vapour deposition PVD process in which high energetic particles like an ions, an electrons, an alpha particle etc are targeted on the surface with enough energy to eject atleast one or more surface atom and depositing these sputtered atoms on the substrate. Sputter yield is the ratio of number of ejected atoms to the number of incident atoms.

#### 2.3 DC diode sputtering:

In DC diode sputtering, a discharge between the target and the substrate under suitable pressure (1 to 10 m Torr ) and voltage conditions. Electrical neutral argon gas is introduced into the low pressured vacuum chamber. The DC voltage between the target and substrate ionize the argon gas into plasma resulting into ions and electrons. These charged argon ions are accelerated towards the target/anode. After collision with target it helps to eject atoms from target. These sputtered atoms are than deposited on the substrate/cathode,

resulting deposition of a thin film of target atom on substrate. Electrons released during argon ionization are accelerated towards anode and in the way collides with more argon resulting more argon ion and electrons production. The applied voltage required for the discharge is a function of electrode spacing and pressure between them [47]. Figure 2.1 below describes the structure of DC diode sputtering. . To increase the cross section for electron impact and ionization of gas in the chamber it is usually operate at high pressure. But the high pressure results in poor transport of the sputtered atoms and very low deposition rate.

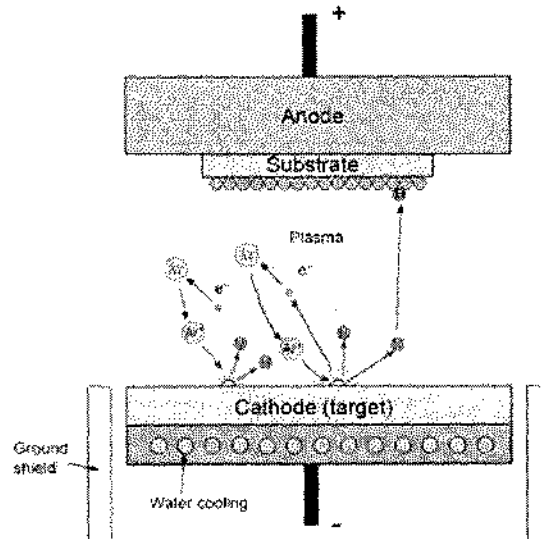


Fig.2.1: Structure of basic DC diode sputtering system.

#### 2.4 RF diode sputtering:

The problems arose in DC sputtering is resolved by applying alternating voltage between the electrodes, in this way charging of insulated cathode is eliminated and also produce an increase in ion current density. In RF diode sputtering mostly AC frequency used is 13.56 MHz. At this frequency plasma oscillates and electrons in the plasma pick additional energy from this oscillation. In this way the energy is coupled into electron population which results in more ionization.

The higher ionization mean production of a higher ion current at the same applied power as that in DC diode sputtering. The second advantage of RF diode sputtering is that by switching the places of anode and cathode at every half cycle of RF, the cathode does not gain charge from plasma. Figure 2.2 describe the structure of RF sputtering system.

## RF Sputtering

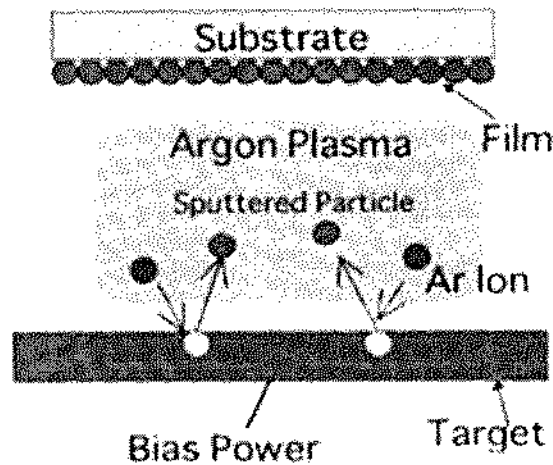


Fig. 2.2: Basic structure of RF sputtering system.

In RF diode sputtering, both etching and deposition is commonly used for the sputtering of insulating materials such as oxides (silicon dioxide, magnesium oxide, titanium dioxide, aluminum oxide etc.) and polymers.

### 2.5 Magnetron sputtering:

Synthesis of thin films multilayers is done by magnetron sputtering. It uses the basic effect that electrons respond to magnetic field by the relation,

$$F = e (V \times B) \quad (2.1)$$

Where 'e' is the electron charge, V is the velocity, B is the magnetic field and F is the force acting on electron to spiral around the magnetic field in order to increase the probability of impact with gas atom and cause ionization of gas atom, this in turn produces higher plasma densities and lower discharge voltages at constant applied power [48-54]. Magnetron sputtering system consist of a chamber which is placed in a vacuum. There are two types of chamber with sputtering up or sputtering down phenomena. Vacuum chamber consist of cathode plate and cylindrical anode. A substrate is placed into the chamber. Argon gas is injected into the chamber continuously. Strong magnetic fields are produced by the magnet placed under the target help to deposit target on a confined place at substrate. Now high voltage is applied to ionize argon gas and it will form plasma. During this whole process the electrons ejected from the target will strike with argon gas to form positively charged argon ions. These ion travel to the cathode target and stick with target material. Now these ejected target atoms will move towards the substrate and condenses on the substrate to form a thin film layer. Figure 2.3 describes the whole phenomena.

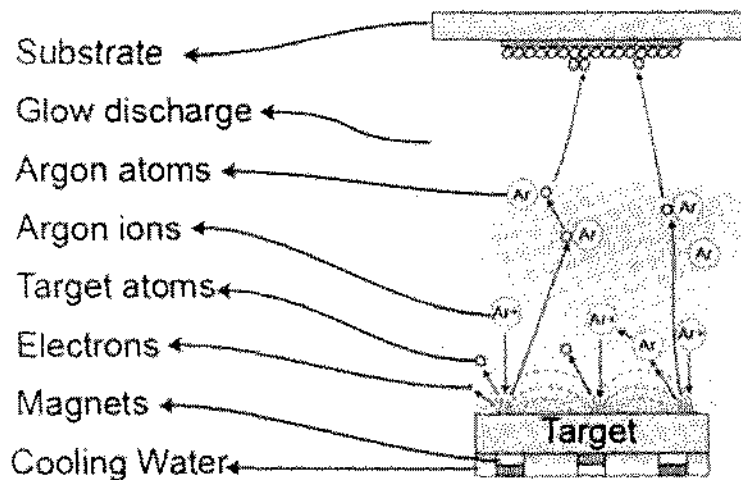


Fig.2.3:Showing Basic components of Magnetron sputtering system.

The rotating substrate stage avoids substrate heating to temperature in excess of 900C with RF or DC bias. A dry backing pump and electro pneumatic valving is computer controlled to provide automatic pumping of the chamber. All process parameters like gas handling, magnetron power supply, chamber and substrate controlled and monitored by lab view software. Deposition from single and multi-sources can be done easily and it depends on sputtering efficiency of the material, deposition power level, source to substrate distance, process gas ,substrate temperature, target erosion, position of anode, process pressure, power type DC/RF, angle of incident and balance of magnetic field.

## 2.6 UV Lithography:

Photo or UV lithography is a process in which portion of a film or the bulk can be selectively removed by using UV rays. In lithography light is used to transfer a geometrical pattern from photo mask to a light sensitive resistor called photo resistor on the substrate and then etched out of the film chemically or physically. Mask lithography is used with coherent light sources and there are two types of mask lithography one is called contact lithography and other is called projection lithography. In contact lithography the mask is placed as closed as possible to the substrate to remove the selected film. This lithography allows us to go below the wavelength limit by keeping precise distance between the film and the mask and helps to create evanescent wave through a hole which are smaller than the applied wavelength. This technique is widely used in industries for the manufacturing of integrated circuit and semi-conductor components. The figure below explains the patterning by photolithography.

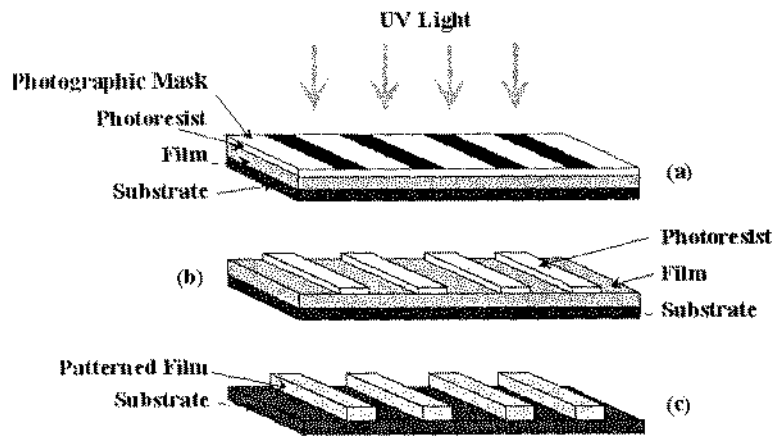


Fig. 2.4: Diagram representation of three stages involved in photolithography.

In first step the clean film is coated with organic photosensitive resistor and allowed to dry before exposed to UV light through a photographic mask to transfer geometrical pattern on the film shown in (fig 2.4a).

In second step the part of resistor that is exposed to UV light become unstable and removed after developing in a photo resist developer for optimal time and shown in (fig 2.4b), when the pattern is done the uncovered film is removed by etching[55-56].

In third step the remaining photoresist is removed by dipping in suitable solvent shown in (fig 2.4c).

## 2.7 Ion-beam etching:

Ion beam etching(IBE) is basically a dry etch process and a transfer of momentum between the incident ion and target atom. In this process the argon ions are radiated on the surface with sufficient energy. The energy of argon ion helps to strike out material of the surface. The striked out material and gas are exhaust by vacuum pump to avoid deposition on walls and sample. As the sputtering yield is the number of sputtered atoms per unit incident ion so it depends upon incident ion energy, species and its mass, target atoms species and mass, and incident angle.[57-58]. The incident ion kinetic energy must be greater than the chemical binding energy of target atom to eject atom from the target and incident energy ranging from 10 to 100KV or depends upon type of target material.

Etching rate(R) is a function of sputtering yield(S) and written as

$$R(\theta) = 9.6 \times 10^{-25} \times J \times (S(\theta)/n) \times \cos(\theta) \quad (2.2)$$

Where J is current density, n is atomic number density and  $(\theta)$  is the angle of incident with normal. As angle increases the sputtering yield increases due to the efficient momentum

transfer between ion and target. In this process only a fraction of incident ion energy is carried away by sputtered atom. By cooling the substrate etching rate can be increased.

## 2.8 Vibrating Sample Magnetometer (VSM):

The Vibrating Sample Magnetometer (VSM) is an instrument invented by Simon Foner in 1955 [59-60] at Lincoln laboratory MIT and is widely used in determining the magnetic properties of various magnetic materials like diamagnetic, paramagnetic, ferromagnetic, and anti-ferromagnetic materials. The VSM system consists of an electromagnet which provides a magnetizing field (DC). In the presence of magnetic field a vibrator that vibrates the sample sinusoidally with the help of piezoelectric material and the detection coils which generate signal voltage due to the change in magnetic flux originates from the vibrating sample. The magnetic moment of sample is proportional to the induced voltage in the pickup coils and can be measured using lock-in amplifier as shown in figure 2.5.

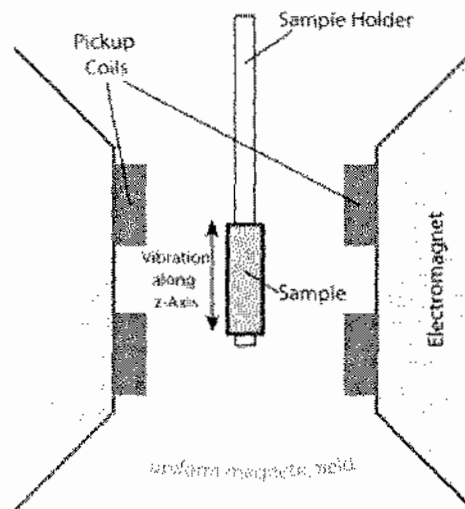


Fig.2.5: Structure of VSM.

This output exhibits the magnetic moment  $M$  as a function of the magnetic field  $H$  and used to obtain the hysteresis curve of material. In this way the VSM measures the magnetization of nanomaterials when placed in external magnetic field and converting the dipole field of sample into AC signals.

---

## Chapter 3

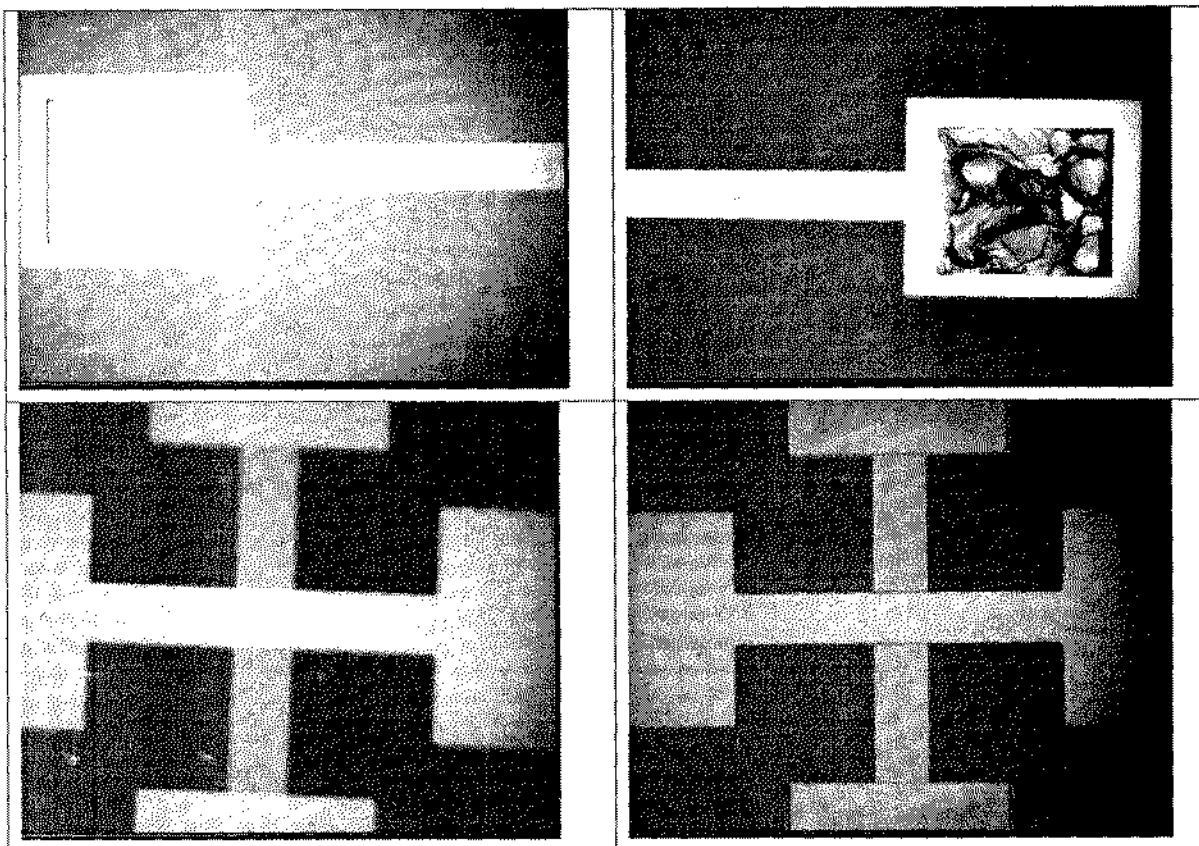
### Experimental techniques

In this chapter different experimental techniques are used for the characterization of magneto tunnel junction nano-materials.

#### 3.1 Optical Microscope:

Optical microscope is technical device used to visualize microscopic things with the help of light. The table below shows few images taken through optical microscope.

Table 3.1 Images by Optical microscope.



#### 3.2 Scanning Electron Microscopy:

Scanning electron microscopy is important characterization techniques for detail study of structure of material. Scanning electron microscope gives information about particle size distribution, morphological structure, grain size and material surface analysis. Main advantage of scanning electron microscopy over XRD is that SEM shows direct image of materials.

Scanning electron microscopy is similar to optical microscopy. Beam of electron is emitted heated filament or by electron tunneling source in scanning electron microscope. Electric field is used to control the movement of beam of electrons so that these electrons gain kinetic energy and short wavelength. For accurate results the beam of electrons passes through large number of series of electromagnetic lenses. Two types of microscopy are used for structural analysis, scanning electron microscopy (SEM) and transmission electron microscopy (TEM). Scanning electron microscopy (SEM) is used in my present research work. Scanning electron microscopy is used to produce high resolution three dimensional images which are helpful for morphology of materials. Beam of electrons emitted from sample surface and collected and amplified with help of detector by using scanning electron microscope. Back scattered and secondary electrons give important information about sample. In order to avoid any distortion in scanning electron microscope the surface of scanning electron microscope (SEM) should be grounded. Fig 3. 4 shows schematic diagram of SEM.

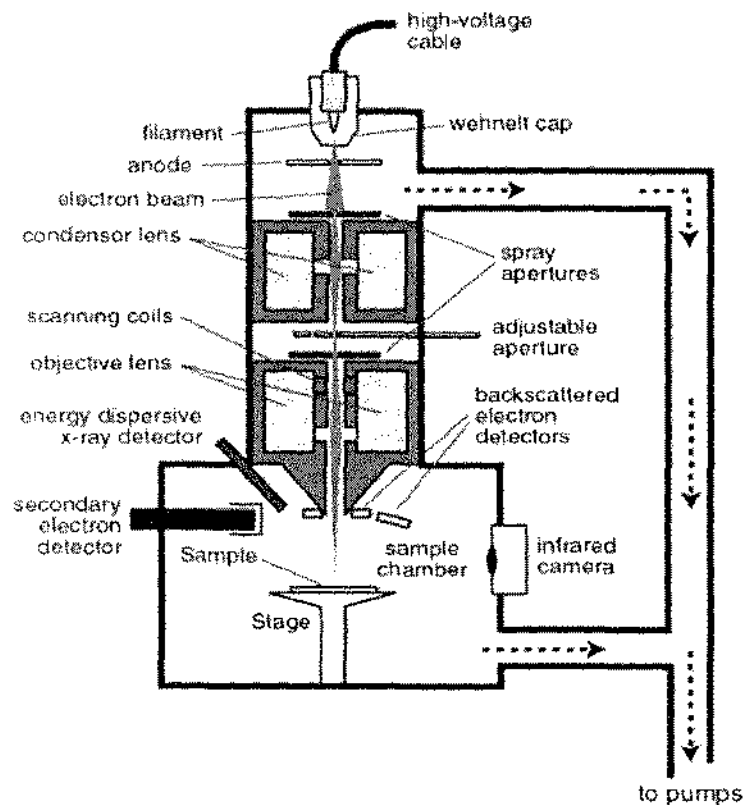


Fig. 3.4: Schematic diagram of Scanning electron microscope [61]

There are different parts used in scanning electron microscope such as heated filament, conducting lens, objective lens, an electron gun and aperture. Electrons are emitted from electron gun in scanning electron microscope and these electrons are accelerated by



gaining kinetic energy and applying high voltage 100 eV to 100KeV between heated filament and anode. Emitted electrons acquired greater kinetic energy in scanning electron microscope which produces a variety of pulse of signals. Backscattered electrons, diffracted electrons, secondary electrons, heat, visible light and photons are parts of these pulses of signals. Backscattered and secondary electrons are used for production of image of specimens.

To show the topography and surface morphology of the thin films, secondary electrons are useful. Backscattered electrons are used to determine the element composition in the thin film. The power magnification of SEM varies from 20X to 50000X and resolution is from 50nm to 100nm. The resolution of SEM is adjusted by the spot size of electron which depends on the electron wavelength.

Vacuum condition is applied for the operation and the image production in SEM, for this the sample should be conductive. If it is non-conductive then sputter coating of metal like Cu is used to make it conductive.

### 3.3 Two Point Probe Method:

For measuring resistance in conductors two probe and four probe method is used. In two probe method the resistivity of sample can be measured by measuring current and potential difference across it as shown in fig (3.5).

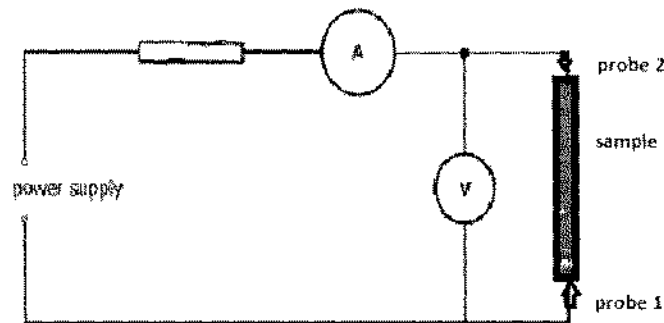


Fig 3.5: Setting of two probe system

In two probe method the current is supplied in through probe 1 across the sample and out from probe 2 is measured by ammeter. The potential difference between the two probes is measured by voltmeter, then the resistivity can be calculated by formula below, where  $l$  is the length of sample between the probes and  $A$  is the cross section of sample.

$$\rho = \frac{V A}{I l} \quad (3.3)$$

#### 3.3.1 Problems of two probe method:

- 1) Increase in resistance due to the contact of measuring lead connection
- 2) It cannot be used for irregular shapes

- 3) It is difficult to solder some materials with lead contact like nanomaterials
- 4) While soldering the heating of sample like semi-conductors result in injection of impurities into material and affect the electrical property.

To overcome these above mentioned problems four point probe technique is used to measure the resistivity of nanomaterials of variety of shapes and also the soldering contacts are replaced by pressure contacts to avoid heating of sample.

### 3.4 Four point probe method:

In this technique four tungsten metal tips with finite radius and supported by springs are used, which are equally spaced as shown in figure (3.6). The springs help to avoid damage caused by the probes to the sample and can easily move up and down while taking measurements.

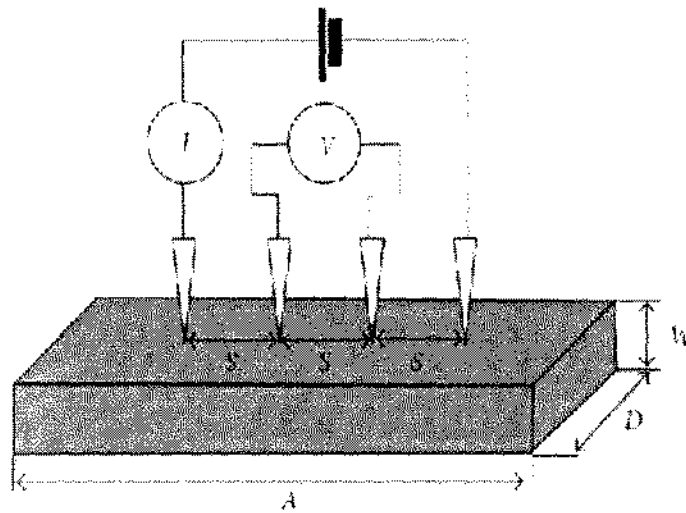


Fig 3.6: Diagram of four point probe setting.

High impedance current is supplied by the source connected to outer two probes 1 and 4. The potential difference is measured by the voltmeter connected across the inner two probes 2 and 3 to determine the resistivity of sample. Usually spacing ( $s = 1\text{mm}$ ) is adjusted between four probes.[62-63]

Due to the high input impedance of voltmeter in the circuit, the current does not draw through inner probes. And the unwanted potential drop caused by contact resistance between the contacts 2,3 probe and sample is eliminated by measuring the potential difference. The resistivity can be formulated by a formula mentioned below.

$$\rho = \frac{V}{I} 2\pi s \quad (3.4)$$

### 3.4.1 Measuring resistance of MTJ by Four point Probe method:

For measuring current in plane tunneling properties of MTJ's like high TMR, low RA product and electronic structure etc, the useful and effective way is four point probe method.

Four small probes are placed on the top of junction stack as shown in fig (3.7). Current is sent by outer two probes and the potential drop is measured by inner two probes to determine the resistance of junction.[64]

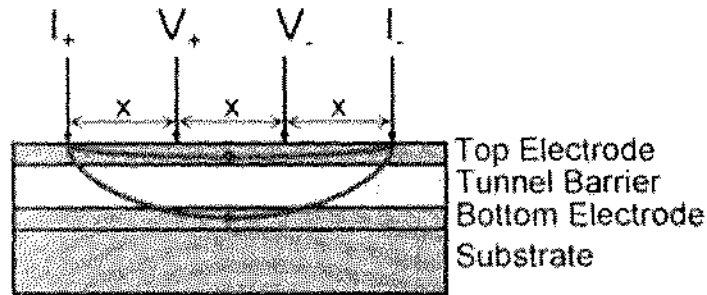


Fig 3.7 : Schematic representation of current in plane tunneling method by four point probe.

A part of current also move cross the barrier and flow through the bottom electrode. Amount of current that flow through bottom electrode depends upon the probe spacing, if the spacing is very close the all of the current flow only through the top electrode and if the spacing is large then the current in top and bottom electrode will flow in a proportion depending on probe spacing. So the distance between the probes is very important to adjust.

The resistance of tunnel junction can sufficiently measure by varying the probe spacing, in this way characteristics of tunnel junction with different barrier thickness can be measured without analyzing the whole pattern of junction.

---

barrier increases the mobility of s-type electrons which leads the spin current in magnetic tunnel junction [65-66].

#### **4.2 Fabrication Of Magnetic Tunnel Junction:**

Fabricating MTJ is done by Top-down method in which different steps like lithography, etching, lift off process etc are carried one by one.

##### **4.2.1 Step 1: Fabrication of bottom electrode**

- i) Positive resistor is pasted on sample to pattern bottom electrode.
- ii) Spinning the sample for suitable time and speed to get uniform resistor distribution on sample
- iii) Baking the sample at 90C for time 1 min in order to get more uniformity of sample and also to remove impurities/ vapours from the surface of sample.
- iv) UV mask lithography is used to paste strongly the resistor on the desired part so that it is protected during etching process.
- v) Resistor exposed to the UV light of suitable wavelength becomes unstable and easily removed after developing in a photo developer for time 35-40 sec and in water for time 20-25 sec.
- vi) Etching is used to remove unnecessary film, which are uncovered by the resistor.
- vii) After etching the sample is dipped in acetone and put in ultrasonic bath for some time in order to remove the resistor.

So after finishing the first step successfully, the bottom electrode is composed

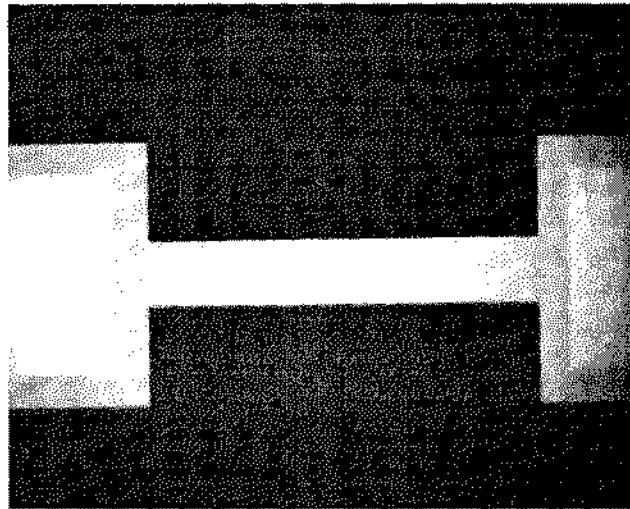


**Fig: 4.2** Shows the fabricated bottom electrode.

#### 4.2.2 Step 2: Fabrication of tunnel junction:

In step 2 fabrication of MTJ is accomplished by pasting negative resistor on the sample. The negative resistor become unstable when exposed to UV light and then the region which is exposed to UV light is easily etched; as soon the etching is finished  $\text{SiO}_2$  is deposited on the sample. As shown in below figure 4.3

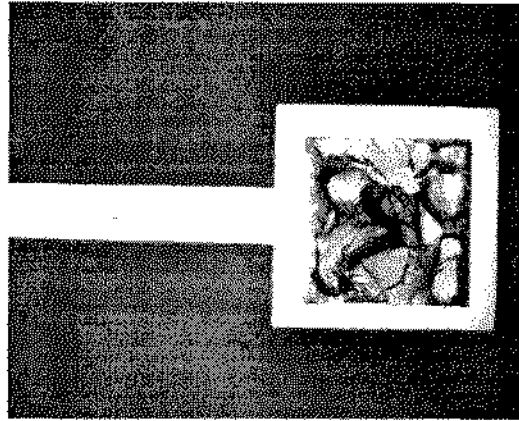






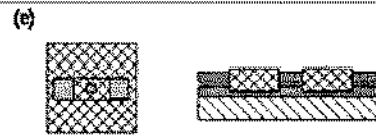
Fig 4.3: Appearance of  $\text{SiO}_2$  depositions on the sample

This helps to shield top electrode from bottom electrode and the junction. All the above stages are described in table 4.1

Table 4.1 Stages of fabrication

(a) Multilayers on substrate.	<p>(a)</p>  <p>Magnetic films Al-O</p>
(b) Sample after UV lithography.	<p>(b)</p>  <p>Resistor</p>
(c) Etching process.	<p>(c)</p>  <p>Ar ion etching</p>
(d) Deposition of $\text{SiO}_2$	<p>(d)</p>  <p><math>\text{SiO}_2</math></p>

(e) After liftoff process.



#### 4.2.3 Step 3: Fabrication of Top Electrode:

After removing unnecessary SiO<sub>2</sub> by lift off process the Cu is deposited to pattern top electrode same as done in step 1.

- i) Positive resistor is pasted on sample to pattern top electrode.
- ii) UV mask lithography is used to paste strongly the resistor on the desired part so that it is protected during etching process.
- iii) Etching is used to remove unnecessary film, which are uncovered by the resistor.
- iv) After etching the sample is dipped in acetone and put in ultrasonic bath for some time in order to remove the resistor.

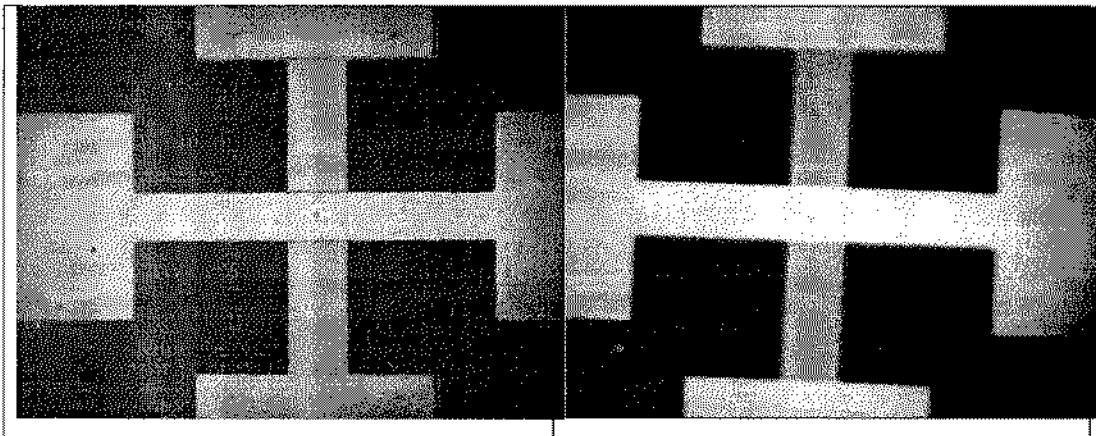


Fig 4.4: (a) left shows sample before dipped in acetone. (b) Right shows sample after dipped in acetone

### 4.3 Transport Properties of CoFeB/Al-O/FeB:

#### 4.3.1 TMR Ratio in AlO<sub>2</sub> Based Magnetic Tunnel Junction:

To calculate the TMR ratio of SBMTJ structure which is deposited on SiO<sub>2</sub> substrate we use four probe technique by applying small dc biased potential difference of +1mV at room temperature and measured the junction resistance that depends upon the applied external field along the plane of MTJ.

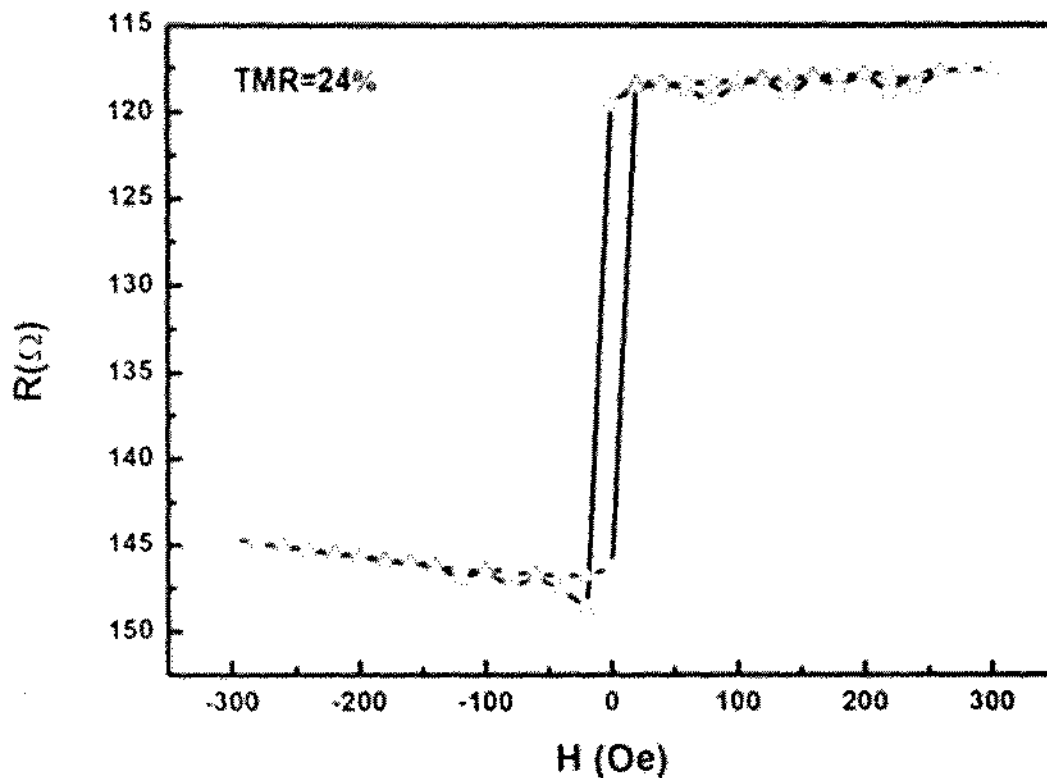


Fig: 4.5 Resistance Curve of SBMTJ before MF annealing at room temperature.

#### Exchange bias for Pinning of ferromagnetic layer:

Figure 4.5 describes the tunneling magneto resistance value that is 24% before magnetic field annealing when electrodes are aligned parallel or anti-parallel state and the curve clearly explain the switching of free electrode. The switching field of two Ferromagnetic electrodes are different and depends upon it coercivities. After fixing the orientation of fixed/pinned layer the magnetic field is applied in the plane and flips the orientation of free layer either parallel or anti parallel position. To avoid the orientation of pinned layer the anti-ferromagnetic layer is used for exchange coupling effect and this effect helps to find maximum resistance.

#### 4.3.2 Magnetic Field Annealing Effects in CoFeB/Al-O/CoFeB MTJ:

In figure 4.6 it is observed after annealing the sample at 265C which is optimized temperature in the presence of 400 Oe magnetic field. The value of TMR ratio increases from 24% to 38% in the same applied conditions due to the following factors,

- (i) Improvement of ferromagnetic layer/barrier interface.
- (ii) Enhancement of the magneto crystalline anisotropy of magnetic layers.
- (iii) Tunneling of mobile electrons

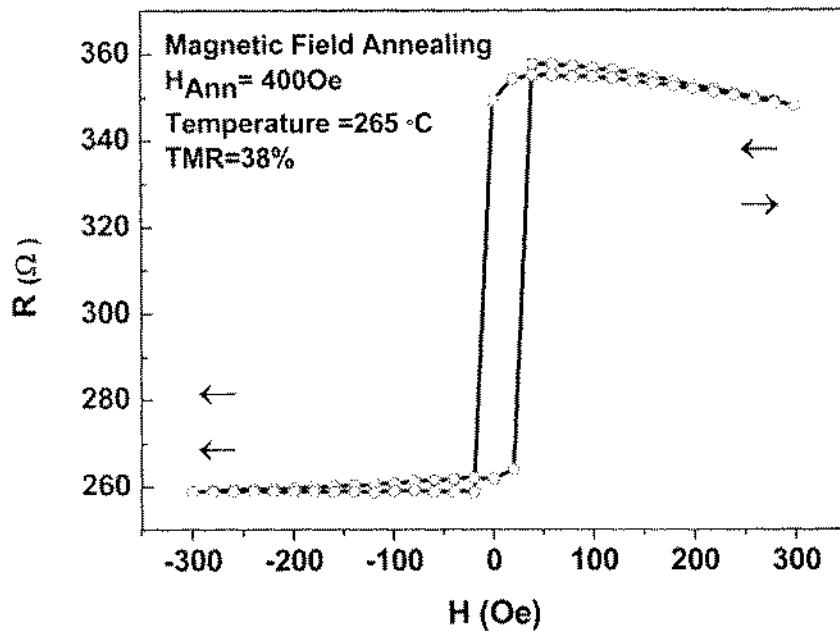


Fig 4.6 TMR curve at room temperature after MF annealing

#### 4.4 I-V Characteristic Curve:

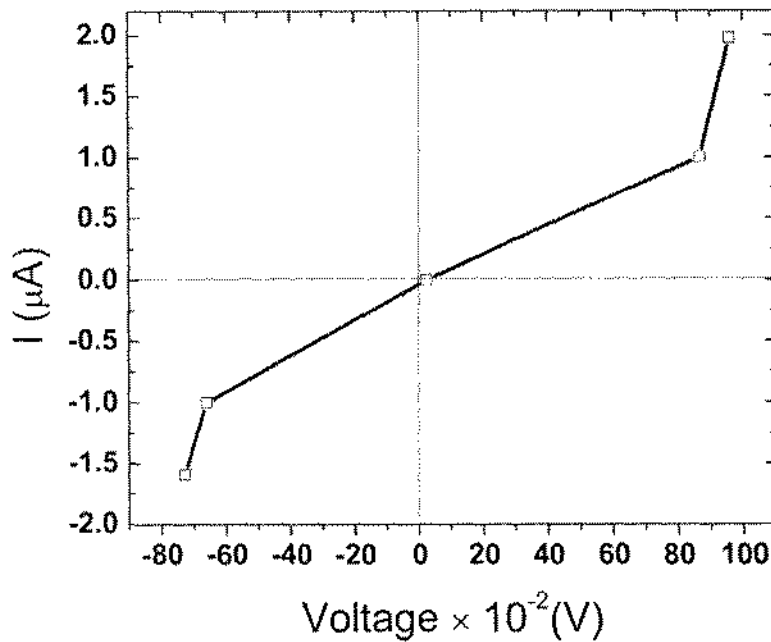


Fig 4.7 Non-Linear I/V curve of SBMTJ at room temperature for anti-parallel state.

We use four probe technique and measured the resistance of SBMTJ in anti-parallel state at room temperature by plotting I/V curve and obtained a nonlinear graph by measuring potential difference across the junction. The IV curves are measured at room temperature to



---

determine the resistance of MTJ's, moreover it is observed from the IV curves that the curve is nonlinear which shows that the resistance is non ohmic and also justifies the tunneling process in MTJ's. This kind of trend in IV curves can be fitted well with the Simmon's model. The figure 4.7 above shows the I/V curve of SBMTJ.

---

## Conclusion

Magnetic Tunnel Junctions Ru5(73.4s)/Cu20(132s)/Ru5(73.4s)/IrMn10(176s)/CoFe2.5(47s)/Ru0.8(12s)/CoFeB3(69s)/Al1nm-Ox(60s)/CoFeB4(91s)/Ru10(146.8s)Ta5(81s)/CoFe8(149.5s)/IrMn10(176s)/Ta3(48.8s) have been prepared by magnetron sputtering system, Ion beam etching and photolithography on SiO<sub>2</sub> substrate in a base pressure of  $P=10^{-8}$ Torr. The IV curves and Tunneling Magnetoresistance (TMR) are measured at room temperature with the help of four point probe method. It is observed from IV curves that the resistance of the MTJ is  $\sim 115\Omega$ . The TMR of the MTJ is found to be 24% when a magnetic field of 300 Oe is applied in the plane of MTJ at room temperature. The MTJs were annealed in the magnetic field  $H_{\text{ann}}=400$  Oe at Temperature  $=265^{\circ}\text{C}$  for one hour. It is interestingly observed that TMR increases from 24% to 38%. The increase in TMR is attributed to smoothing of the interface and crystallinity of the ferromagnetic layers. Beside this IV curves are fitted with the Simon's model. The experimental values from the IV curve are fitted well with the model and barrier height is found in the range of few eV.

## 4.5 References:

- [1] V.Kumar, A.Rana,M.S. Yada, and R.P. Pant, J.Mang. Mang.Mater.**320,1729** (2008)
- [2] S.Araki,J.Appl.Phys.**73,3910-3916**(1993)
- [3]B.G.Park,J.Wunderlick,D.A.Williams,S.j.Joo,K.Y.Jung,K.H.Shin,K.Olenjnik,A.B.Shick,T.Jungwirth,Phys.Rev.Lett.**100,087204-087207**(2008).
- [4] Soshin Chikasaki, "Physics of Magnetism" John Wiley and Sons, (1964).
- [5] B. D. Cullity, "Introduction to Magnetic Materials", Addison-Wesley Publishing, (1972).
- [6] Nicola A. Spaldin, " Magnetic Materials: Fundamentals and Device Applications", Cambridge University Press, (2003)
- [7] I. I. Oleinik, E. Y. Tsymbal, D. G. Pettifor, Phys. Rev. B **62, 3952** (2000).
- [8] S. Ikeda, J. Hayakawa, M. L. Young, F. Matsukura, Y. Ohno, T. Hanyu, H. Ohno, IEEE Trans. Elec. Devices. **54, 991** (2007).
- [9] Introduction to electronic nanotechnology and quantum computing by Prof Edward I Wolf.
- [10] J. Schmalhorst, S. Kämmerer, G. Reiss, A. Hütten, Appl. Phys. Lett. **86, 152102** (2005).
- [11] Y. Luo, K. Samwer, J. Mag. Magn. Mater. **240, 156** (2002).
- [12] C. Chappert, A. Fert, F. N. V. Dau, Nat. Mater. **6, 813** (2007).
- [13] S. Yuasa, T. Nagahama, Y. Suzuki, Science **297, 234** (2002).
- [14] P. V. Paluskar, J. J. Attema, G. A. de Wijs, S. Fiddy, E. Snoeck, J. T. Kohlhepp, H. J. M. Swagten, R. A. de Groot, B. Koopmans, Phys. Rev. Lett. **100, 057205** (2008).
- [15] Y. Wang, Z. M. Zeng, X. F. Han, X. G. Zhang, X. C. Sun, Z. Zhang, Phys. Rev. B **75,214424** (2007).
- [16] B. S. Berry, W. C. Prothet, Phys. Rev. Lett. **34, 1022** (1975).
- [17] H. X. Wei, T. X. Wang, Z. M. Zeng, X. Q. Zhang, J. Zhao, X. F. Han, J. Mag. Magn. Mater.**303,e208** (2006).
- [18] J.S. Moodera, L.R. Kinder, T.M. Wong, and R. Meservey. Large magnetoresistance at room temperature in ferromagnetic thin film tunnel junctions. *Phys. Rev. Lett.*,**74:3273–3276**, 1995.
- [19] T. Miyazaki, N. Tezuka, J. Mag. Magn. Mater. **139, L231** (1995).
- [20] J. S. Moodera, L. R. Kinder, T. M. Wong, R. Meservey, Phys. Rev. Lett., **74,3273** (1995).
- [21] S. Jin, T. H. Tiefel, M. Mc Cormack, R. A Fastnacht, R. Ramesh, L.H Chen,Science **264, 413** (1994).
- [22] R. Von Helmut, J. Wecker, B. Holzapfel, L. Schultz, K. Samwer, Phys. Rev. Lett. **71, 2331** (1993).
- [23] A. M. H-Gosnet, J. P. Renard, J. Phys. D: Appl. Phys. **36, R127** (2003).
- [24] T. Miyazaki, T. Taoi, S. Ishio, J. Magn. Magn. Mater. **98, L7** (1991).
- [25] E. Y. Tsymbal, O. N. Mryasov, P. R. LeClair, J. Phys. C. Condens. Matter. **15, R109**(2003).
- [26] T. Miyazaki, N. Tezuka, J. Magn. Magn. Mater. **151, 403** (1995).
- [27] J. S. Moodera, L. R. Kinder, T. M. Wong, R. Meservey, Phys. Rev. Lett. **74, 3273**(1995).
- [28] X. Liu, D. Mazumdar, W. Shen, B. D. Schrag, G. Xiao, Appl. Phys. Lett. **89, 203504**(2006).
- [29] X. Liu, D. Mazumdar, B. D. Schrag, W. Shen, G. Xiao, Phys. Rev. B **70, 014407** (2004).
- [30] X. Liu, C. Ren, B. D. Schrag, G. Xiao, L. F. Li, J. Magn. Magn. Mater.**267**(2003) 133.
- [31] S. Machlup, J. Appl. Phys. **25, 341** (1954).
- [32] L. I. Maissel, R. Glang, Handbook of Thin Film Technology, Mc-Graw Hill, (1970).

- 
- [33] A. P. Malozemoff, A. R. Williams, V. L. Moruzzi, K. Terakura, Phys. Rev. B **30**, 6565(1984).
- [34] De Groot, R. A. Muller, F. M. van Engen, P. G. Buschow, K. H. J. Phys. Rev.Lett. **50**, 2024 (1983).
- [35] D. G. Wingett, K. Forcier, C. P. Nielson, J. Mag. Magn. Mater. **192**, 203 (1999).
- [36] M. Kiwi, J. Mag. Magn. Mater. **234**, 584 (2001).
- [37] A. E. Berkowitz, K. Takano, J. Mag. Magn. Mater. **200**, 552 (1999).
- [38] R. L. Stamps, J. Phys. D: Appl. Phys. **33**, R247 (2000).
- [39] F. S. Bergeret, A. F. Volkov, K. B. Efetov, Rev. mod. Phys. **77**, 1321 (2005).
- [40] A. I. Buzdin, Rev. Mod. Phys. **77**, 935 (2005).
- [41] B. Dieny, V. S. Speriosu, S. S. P. Parkin, B. A. Gurney, D. R. Wilhoit, D. Mauri, Phys.Rev. B **43**, 1297 (1991a).
- [42]Grancharov S G ,zeng h,sun s,et al.Bio functionlization of monodisperse magnetic nano particles and their use as bio molecular labels in magnetic tunnel junction based sensors.j physics chem B,2005,109;13030-13035.
- [43]Shen W,SchrangBD,CarterMJ,et al. Quantitative detection of DNA labeled with magnetic nanoparticles using array of MgO-based magnetic tunnel junction sensors.Appl phys let,2005,93:033903.
- [44] P. Sigmund, Phys. Rev. **184**, 383 (1969).
- [45] P. Sigmund, Phys. Rev. **187**, 768 (1969).
- [46] P. C. Zalm, Surface and Interface Analysis **11**, 1(1988).
- [47] D. M. Hoffman, B. Sing, J. H. Thomas, '*Handbook of vacuum science and technology*' Academic Press 1998.
- [48] D. Flamm, G. Herb, '*Plasma etching: An introduction*' D. Mannos, D. Flamm Academic Press 1989.
- [49] H. S. Butler, G. S. Kino, Phys. Fluids, **6**, 1346 (1963).
- [50] K. Riemann, J. Appl. Phys. **65**, 999 (1989).
- [51] M. A. Liberman, IEEE Trans. Plasma Sci, **PS-17**, 338 (1989).
- [52] D. Vender, R. Boswell, J. Vac. Sci. Tech. **A10**, 1331 (1992).
- [53] P. M. Vallinga, P. M. Meijer, F. J. de Hoog, J. Phys. D. Apply. Phys. **22**,1650(1989).
- [54] G. R. Misium, A. J. Lichtenberg, M. Liberman, J. Vac. Sci. Tech. **A7**, 1007(1989).
- [55]"An automated system for measuring the complex impedance and its relaxation in soft magnetic materials", J.P. Sinnecker, M. Knobel, M.L. Sartorelli, J. Schonmaker, F.C.S. Silva, J. de. Phys. IV Vol.8 No.(2). 665 (1998).
- [56]"An introduction to physics and technology of thin films", A. Wagendristel, Y. Wang, World Scientific Publishing, pp31-40, (1994).
- [57] K. Marutama, S. Endo, G. Sasaki, K. Kamata, J. Nishino, K. Kuchitsu, J. Mat. Sci.Lett. **11**, 1588 (1992).

- 
- [58] H. S. Kwok, *Appl. Phys. Lett.* **59**, 3543 (1991).
- [59] S. Jashree, R. Padiyah, T. H. Rasmussen, S. V. Babu, *Appl. Phys. Lett.* **63**, 473(1993).
- [60] Foner, Simon (1959). "Versatile and Sensitive Vibrating-Sample Magnetometer". *Rev. Sci. Instrum.* **30** (7): 548–557. doi:10.1063/1.1716679
- [61] M. T. Postek, K. S. Howard, A.H. Johnson and K. L. McMichael, Scanning electron microscopy (Ladd Research Ind., Inc. Williston, VT., 1980)
- [62] Smits FM. Measurement of sheet resistivities with the four-point probe. *Bell System Technical Journal.* 1958 ;34:711-718.
- [63] Yi Lu and John R Bowler 2012 *Meas. Sci. Technol.* **23** 115603. doi:10.1088/0957-0233/23/11/115603
- [64] D.C. Worledge and P.L. Trouilloud, *Appl. Phys. Lett.* **83**, 84 (2003)]
- [65] S. Ikeda, J. Hayakawa, M. L. Young, F. Matsukura, Y. Ohno, T. Hanyu, H. Ohno, *IEEE Trans. Elec. Devices.* **54**, 991 (2007).
- [66] C. Chappert, A. Fert, F. N. V. Dau, *Nat. Mater.* **6**, 813 (2007).

# Turnitin Originality Report

MTJs by Faizan Paracha

Similarity Index

12%

Similarity by Source

Internet Sources:	1%
Publications:	8%
Student Papers:	4%

Processed on 18-Feb-2015 12:20 PKT  
ID: 506656841  
Word Count: 9129

## sources:

- 1 2% match (student papers from 11-Jul-2013)  
Class: Quick Submit  
Assignment:  
Paper ID: 340311991
- 2 2% match (publications)  
Han, Xiuhong, Syed Ishaq Ali, and Shiheng Li. "MgO(001) barrier based magnetic tunnel junctions and their device applications". Solid State Physics, Mechanics and Astronomy, 2013.
- 3 2% match (publications)  
S ROSSNAGEL. "High-vacuum-based processesSputtering". Handbook of Vacuum Science and Technology, 1998.
- 4 1% match (publications)  
M POWER. "Elect. Beam Technology". Handbook of Vacuum Science and Technology, 1998.
- 5 1% match (publications)
- 6 < 1% match (Internet from 20-Sep-2014)  
<http://www.pvdproducts.com/sputtering-systems/magnetron-sputtering-systems>
- 7 < 1% match (Internet from 25-Oct-2011)
- 8 < 1% match (publications)

- 9 < 1% match (publications)  
Chen, Peifeng "Spin polarized tunneling and spin injection in Fe-GaAs hybrid structures"  
Publikationsserver der Universität Regensburg, 2006.
- 10 < 1% match (student papers from 17-Apr-2012)
- 11 < 1% match (publications)  
 Hamann, Jorge, and Jorge E. ... Prof. Dr. Bernd G. ... Prof. Dr.  
 Rüdiger ...  
Naturwissenschaften) "Spin polarized tunneling and spin injection in Fe-based materials"  
Sächsische Landesbibliothek - Technische Universität Chemnitz, 2011.
- 12 < 1% match (student papers from 17-Dec-2013)  
 Submitter: to Higher Education Commission Pakistan on 2013-12-17
- 13 < 1% match (publications)
- 14 < 1% match (publications)  
 Wolf, Kurt, and ...  
 2006.
- 15 < 1% match (publications)  
 T. Nozaki, "Quantum Oscillation of the Tunneling Conductance in Fully Epitaxial Double Barrier Magnetic Tunnel Junctions", Physical Review Letters, 01/2006
- 16 < 1% match (student papers from 26-May-2012)
- 17 < 1% match (publications)  
 Kelter, "Components and Properties of Matter", Chemistry An Industry-Based Introduction with CD-ROM, 2000.
- 18 < 1% match (student papers from 30-Oct-2009)
- 19 < 1% match (student papers from 12-Dec-2013)  
 Submitter: to University of KwaZulu-Natal on 2013-12-12